INSTITUTE OF FUNDAMENTAL STUDIES

KANDY SCHOOL OF SCIENCE

WORKSHOP

on

"X-RAY FLUORESCENCE"

THEORY, INSTRUMENTATION AND ANALYSIS

on

23 - 24 September 1993

Conducted by

Dr. G. M. FONSEKA

Senior Lecturer in Physics, Open University of Sri Lanka
and Visiting Scientist, IFS

at the IFS Auditorium, Kandy

Institute of Fundamental Studies
Hantana Road
Kandy
Tel: 08-32002

0120

CONTENTS

Workshop on X-ray Fluorescence Analysis

The purpose of this workshop is to assist young researchers in Sri Lanka to acquire the basic knowledge in X-ray Fluorescence analysis. XRF is globally used in industry and research and a knowledge of XRF is an advantage for geologists, material scientists, environmentalists etc. XRF as an analytical tool is now being increasingly used in Sri Lanka for the analysis of geological, cement, steel ceramic and petroleum materials. Therefore, it is expected that this workshop will be useful to an array of scientists, researchers, and technologists.

I wish to thank the Director of the Institute of Fundamental Studies, Vice-Chancellor and Prof. of Physics of the Open University of Sri Lanka for granting me permission to conduct this workshop.

Long term assistance given by Messrs L. Liyanage, M. Kulatunga is much appreciated and special word of thanks goes to Mr. M.W.K. Weerakoon for his devoted service with XRF in preparation to this workshop.

Finally I thank Ms. Asoka Amarasekera for typesetting the document so efficiently and quickly, and to Messrs R.B. Weerakoon and W.G. Jayasekera for preparing the final camera-ready copy.

G.M. Fonseka

Fundamentals of X-ray Fluorescence (XRF) Analysis

G.M. Fonseka
Open University of Sri Lanka/Institute of Fundamental Studies,
Kandy - September, 1993

Introduction

X-rays were first discovered by Wilhelm Rontgen (1895). Since X-rays undergo diffraction they are a form of waves and is known to occupy a small part of electromagnetic spectrum (Fig.1).

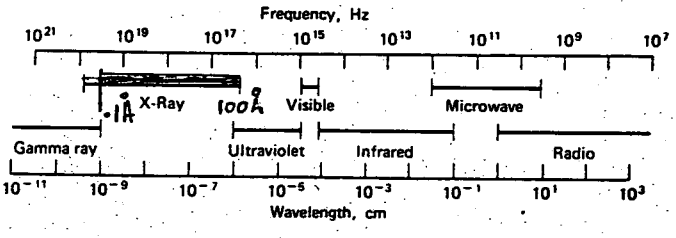

Fig.1 - The electromagnetic spectrum

The X-ray region is normally considered to be in the wavelength (λ) range 0.1-100A^0 (1A^0 = 10^{-10}m). However, 50-500A^0 region is treated as the soft X-ray and vacuum u.v. region. Electro magnetic radiation exhibits not only the wave nature but also the corpuscular nature. The energy of a corpusle (or photon) is $h\nu$ (or hc/λ). Because of this dual nature of X-rays we can identify them with wavelength or with photon energy.

Ever since Moseley showed that each element produced a characteristic X-ray spectrum, it has been possible to use this **'atomic fingerprint'** in non-destructive elemental analysis. However X-ray (powder) diffraction (XRD) porvides a **'structure fingerprint'** of crystalline materials. Both methods involves the dispersion of X-rays. In one case (XRF) according to the wavelength (or energy) of the characteristic radiation emitted by excited atoms, and in the other (XRD) according to the interplanar spacing of a crystal lattice. XRF analysis is, in theory capable of dealing with all forms of matter, whereas diffraction analysis is confined, in the main, to crystalline materials.

The Origin of X-rays

X-rays are usually produced by bombarding a target with high energy electrons (Fig.2). The kinetic energy (U) of the electrons at the heated cathode is negligible, however when reaching the target achieves a kinetic energy equal to e_0V_0. The bombarding electrons can interact with the atoms of the target in a number of different ways. They can suffer deceleration in the electric field of target atoms and emit radiation of varying wavelengths. According to the quantum picture the change of electrons kinetic energy U_f-U_i produces a photon of energy $h\nu$ (or $h\,c/\lambda$). The conservation of energy implies U_f-U_i = $h\nu$ (or $h\,c/\lambda$). The radiation produced in this way is called 'Bremsstrahlung' meaning 'braking radiation' in German. Some call it white radiation.

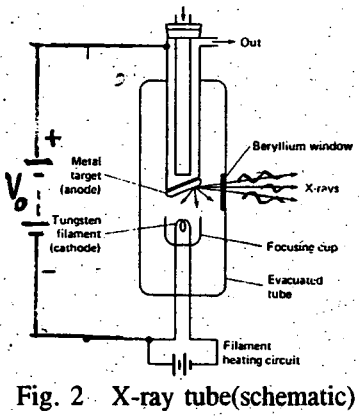

Fig. 2 X-ray tube(schematic)

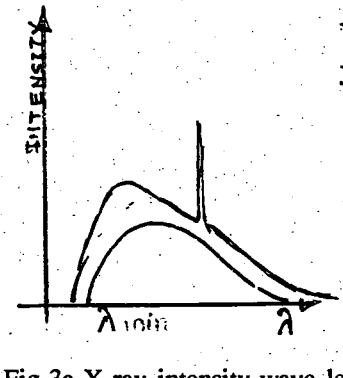

Fig.3a.X-ray intensity-wave length

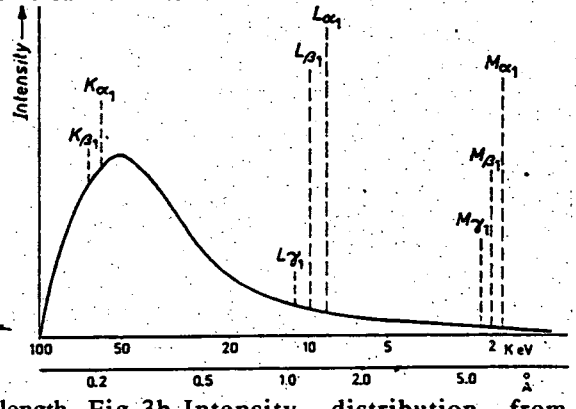

Fig.3b.Intensity distribution from a tungsten X-ray tube at 100 kV.

An electron may produce a number of waves (or photons) before coming to rest. A large number of bombarding electrons produce a statistical distribution of wavelengths (or photon energies) as shown in Figs. 3a, (3b). The most energetic photon possible will occur when an electron looses all of its kinetic energy in a single interaction

producing a single photon with maximum energy (or waves with maximum frequency or minimum wavelength)

$$U_f - U_i = U_f - 0 = e_0V_0 = h\nu_{max} \text{ or } hc/\lambda_{min}$$

Note that the photon with maximum energy has an energy e_0V_0 and is directly identified with the X-ray tube voltage V_0. The Bremsstrahlung process produces a continuous spectrum with a minimum wavelength (λmin). Using known values of h,c,e_0, it can be shown $\lambda_{min} = 12.4/e_0V_0$ where V_0 is now in kilo-volts. The formula is worth memorizing.

It is obvious that the conversion of the whole energy of an electron into a photon is a rare event and the intensity at λ_{min} is very small. It has been found that an electron loosing half of its kinetic energy in a single act is a most likely event; and this produces the most number of photons. Therefore the maximum in the 'white' radiation hump is around $2\lambda_{min}$.

The effect of target material on white radiation

Heavy atoms have a large number of orbital electrons that give a strong internal electric field. Hence the incoming electrons from the cathode can be more effectively decelerated than by light atoms. So efficiency of X-ray production can be increased with heavy targets. However, less than 1% of bombarding electron energy goes for X-ray production and the remainder goes to produce heat. The total intensity of X-rays is proportional to the atomic number (Z) of target. The heat produced in the target must be taken away preferably by a water cooling system.

Production of characteristic X-ray spectra

This is the radiation which Moseley found was characteristic of the target atoms. This discovery led to the Bohr theory of the atom. Very little of subsequent refinements of Bohr model of the atom is required for sufficient understanding of the characteristic radiation in XRF analysis.

Characteristic radiation by electron bombardment

It is possible for energetic incident electrons to eject orbital electrons of the target material. If a core electron is ejected, electrons from higher energy levels in the target atom will make transitions to this lower vacated state, emitting radiation in the process. Since the energy differences among the inner levels of the target atoms are large, the transitions create photons of higher frequency (or shorter wavelength) and belong to the X-ray region. Since the energy differences are characteristic to an atom (depending on its nuclear charge) the wavelength itself is characteristic to the atom, hence the name characteristic wavelength.

$$(E)_{K\alpha} = E_K - E_L$$
$$(E)_{K\beta 1} = E_K - E_M$$
$$(E)_{L\alpha} = E_L - E_M$$
$$(E)_{L\beta 2} = E_L - E_N$$
$$(E)_{M\alpha} = E_M - E_N$$
$$(E)_{K\beta_2} = E_K - E_N$$

If K-shell (n=1) electrons are removed, electrons from higher energy states falling into K shell produces the K series lines (Kα, Kβ; Kα for Δn=1, Kβ for Δn=2 etc. If L-shell (n=2) electrons are removed, another series of lines called L series is produced. Similarly transitions to M shell (n=3) produces M series (see fig. 4).

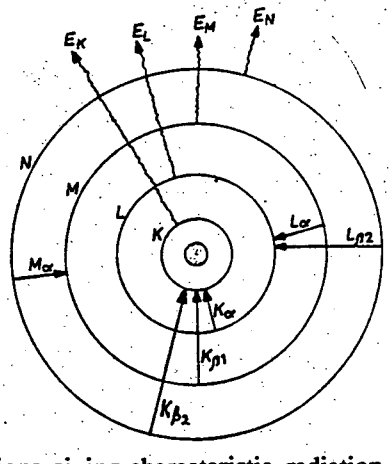

Fig.4 - Transitions giving characteristic radiation

Fine structure of atomic shells, the sub-shells

During the excitation of multi electron atoms by electron bombardment one observes the smooth continuous spectrum (the white radiation) having the short wavelength cut off (λ_{min}) together with intense sharp lines produced by Kα, Kβ, etc. Upon closer examination these lines show that they are composed of finer lines. This is explained by atomic sub-levels. Only the K-shell has a single energy level. All the other shells contain electrons with slightly different energies. The L-shell has 3 sub levels, the M-shell 5, etc. Atomic sub levels gives the fine structure. It should be noted that certain physical rules (selection rules) make certain transitions prohibitive such transitions have a zero probability of occurrence. Once an atom has been ionized, for example, in the K-shell there is a certain

probability that this vacancy can be filled from L_I, L_{II}, L_{III}, M_{III}, etc. The probability for a transition from L_I to K is zero. Similarly many others jumps have zero probability. The well known transitions are $K\alpha_1$, $K\alpha_2$ (from L_{II} & L_{III}), $K\beta_1$, $K\beta_2$, from M_{II}, M_{III}. Note here that the accepted nomenclature of X-ray lines is unfortunately somewhat unsystematic but in general the final resting place of the transferred electron determines the series group to which the line belong (Fig. 5).

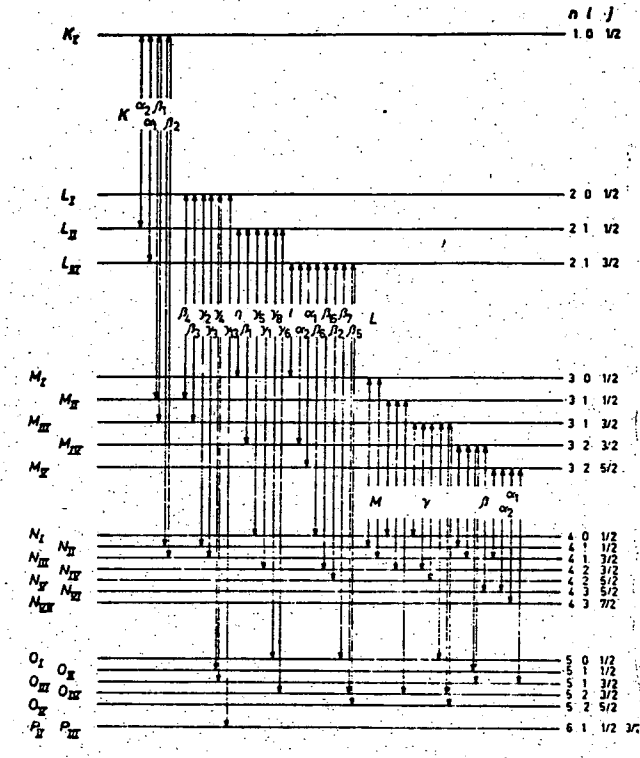

Fig. 5 - The fine structure of the energy levels in the electron shells. The transitions shown are all those theoretically possible. Not more than a dozen are normally detectable in fluorescence analysis. The distance apart of the lines within the shells is some indication of relative energy differences, but the distance between shells is much too small to represent relative energy differences.

The measurement of shell energy E_K, E_L

The shell excitation energies E_K, E_L, etc. can be measured in two ways. Suppose an X-ray tube has a target composed of the element under investigation and a detector is adjusted to register the K radiation from the target. As the voltage is raised there will at first be no response from the detector, until a definite excitation voltage V_{ex} is reached when the first photons will be registered. At this voltage the bombarding electrons are just energetic enough to eject an electron from the K shell so that $E_K = eV_{ex}$.

Intensity of characteristic radiation from electron bombardment

If we increase the acceleration voltage V_0 further, the intensity of the K radiation will increase approximately proportional to $(V_0 - V_{ex})^2$. In other words, the further V_0 is away from V_{ex} on the high energy side the more intense is the characteristic radiation.

Characteristic radiation from photon-bombardment

We can imagine an experiment where monochromatic photons bombard the specimen (instead of electrons). Now vary the wavelength from long to short, i.e. from less energetic to more energetic photons. Until the energy of the photons is equal to E_K, no response will be produced in the detector. Upto this point the results are similar, but at or just beyond this point a large number of $K\alpha$ photons will be produced. This can be easily separated because $E_K > E_K - E_L$ and the bombarding photons have a shorter wavelength than the excited $K\alpha$ photons. As the bombarding photons are made more energetic the response falls (c-f electron bombardment where the response is increased). This is because photon interaction is a resonance effect. **The maximum interaction occurs when the frequences are equal** and declines as the gap between them increases. If $K\alpha$ characteristic radiation to be excited by photon bombardment then the wavelength of the bombarding photon **must be shorter than** that corresponding

to E_K (c.f. electron bombardment).

Intensity of characteristic radiation from photon bombardment

The experiment with photons is difficult to carry out, but an equivalent to the second part of the experiment using monochromatic X-rays from a radio-active source (Cd^{109} giving rise to AgK_α X-rays) is straightforward. The minimum detectable amount of elements of lower atomic number than Ag, using this method of excitation is shown in Fig. 6. The smaller the minimum detectable amount, the more efficient is the excitation process. As can be seen, this falls off rapidly as the gap between the bombarding photon energy and E_K increases.

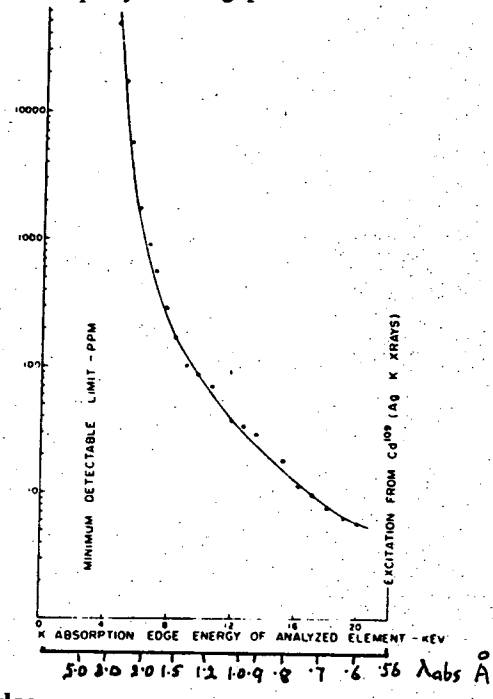

Fig 6 - The efficiency of production of characterictic radiation is inversely proportional to the minimum detectable limit(MDL) of the element concerned

The first part of the experiment with photons - to find the value of E_K - can be more easily carried out using absorption of X-rays. If white radiation is incident on a sheet containing the element being investigated, and the transmitted X-rays analyzed by energy or wavelength, then for wavelengths greater than that corresponding to E_K, no absorption due to K shell excitation can occur. At the wavelength corresponding to E_K, this absorption mechanism suddenly comes into full effect, and a dramatic increase of absorption occurs.

Absorption edge

The curve of transmitted intensity vs wavelengths has a sharp step - **the absorption edge** - at this point, and if λ_{abs} is the wavelength at this absorption edge, $h\nu_{abs} = hc/\lambda_{abs} = E_K$. This absorption edge is also characteristic of the element and can be used for identification (XAFS-Xray absorption Fluorescent Spectrocopy). For L and higher shells there are several absorption edges close together, corresponding to the fine structure of the shell.

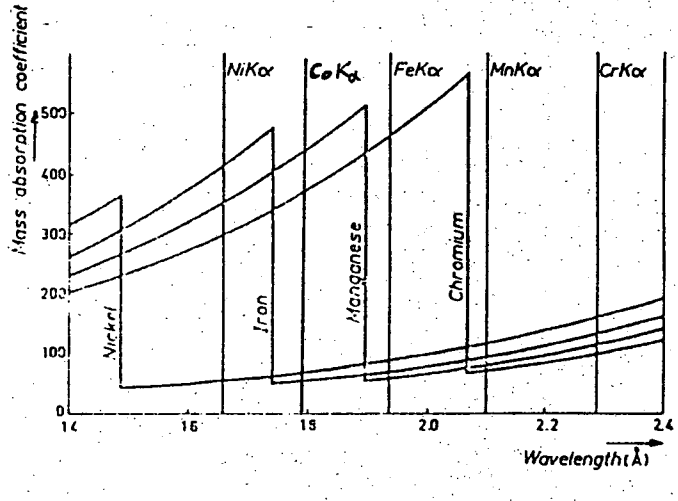

Fig. 7 - Variation of mass absorption coefficient with wave length and origin of absorption and enhancement effect in high alloy steel

The greater advantage of fluorescent excitation - excitation using bombarding photons - is that virtually no background white radiation is produced. The restriction to wavelengths just on the short side of λ_{abs} is not so important as might be thought, because the white radiation from an X-ray tube can be used and a great range of wavelengths is available for exciting different elements. The maximum of the white radiation 'hump' should be adjusted, if possible, on the short side of λ_{abs} for the element to be detected to get adequate excitation.

Auger electrons

The release of energy when an electron moves from higher to a lower orbit can be in the form of a characteristic photon OR may be transferred to an outer electron, to eject it from the atom as an Auger electron with a characteristic energy (which can also be used in the identification of such elements - Auger electron spectrocopy). Production of Auger electrons is more with lighter elements.

Fluorescent yield

An important consequence of the Auger effect is that the actual number of useful X-ray photons produced from an atom is less than would be expected. The Fluorescent Yield is defined as the proportion of ionized atoms which produce characteristic photons. This approaches 100% for heavy elements and becomes very low for light elements

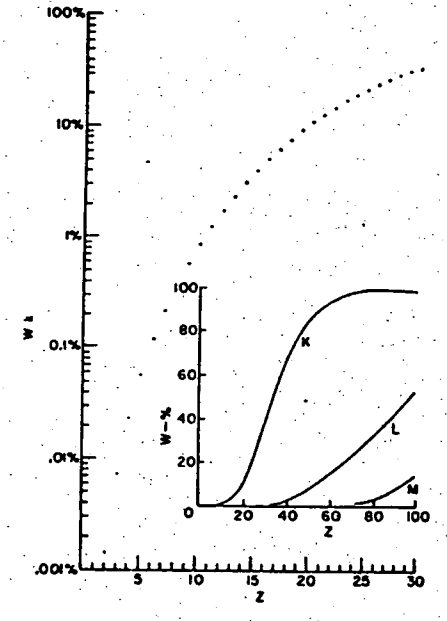

Fig 8 - The fluorescent yield, W is the percentage of excited atoms which decay to give a characteristic photon (the main alternative is an Auger electron). For C, N and O (Z = 6,7 and 8) less than 1% onwards, more than 50% decay giving photons.

Relative intensities of characteristic emission lines

Fortunately only a few of the possible lines have significant intensities. Fig. 3(b) shows the significant lines for tungsten on the white radiation background from an X-ray tube run at 100 kV. The relative heights of the lines are approximately correct, but they have been drawn to a much smaller scale relative to the white radiation, i.e. the lines should be an order of magnitude higher. For a normal tungsten target tube run at 50 kV, the white radiation background would be only about 1/8 the height shown in Fig. 3b and the spectrum would end at 0.25 Å with no K lines. For a Cu target tube, the K lines would be near the position of the WL lines, but much higher. However, in most cases it is not necessary to consider any other lines than those on Fig. 3b, for any individual element, although some of the weaker lines for an element present in large proportions may interfere with the diagnostic lines of a trace element, and have to be taken into account. The abscissae of Fig. 3b are on a log-scale and mask the fact that the energy difference between L and M lines is about 8 KeV whereas between K and L it is 50 KeV. These values get less as one goes down the Periodic Table, but the K-L energy difference is always much greater than L-M, which is greater than M-N, etc. This is shown by the difference between the energies of Kα and Kβ photons, which is the difference in energy between the L and M shells, since Kβ comes from an M-K transition and Kα from L-K. Fig.9 shows the variation of photon energy with atomic number.

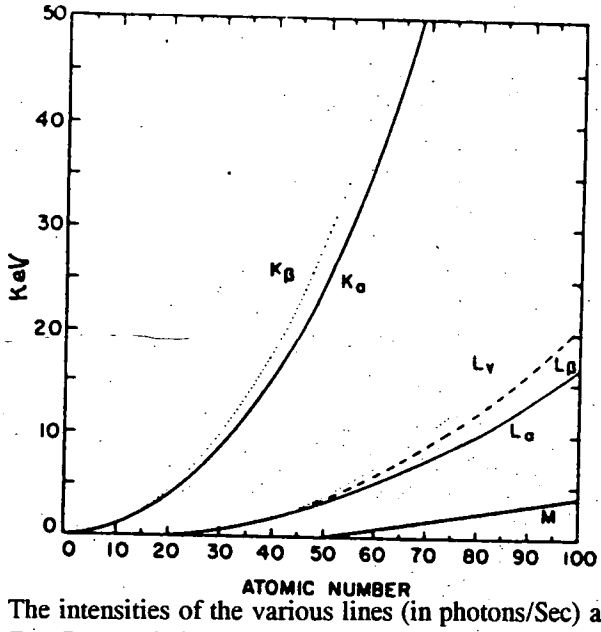

Fig 9 - The photon energies in keV of characteristic lines of the elements.

The intensities of the various lines (in photons/Sec) are proportional to the corresponding transition probabilities. For CuK radiation $I\alpha/I\beta \sim 5$, but this ratio varies gradually from 25 for Al to 3 for Sn.

Fluorescent X-ray tubes

Special X-ray tubes are required to produce radiation for fluorescent excitation. Since for most purposes a large flux of white radiation is required, a high atomic number target must be chosen and W is normally used. The voltage on the tube should be at least twice the excitation voltage of the element in the sample, but although further increase of voltage (at constant power) will continue to increase the white radiation intensity near the absorption edge of the element concerned the gain is proportionately much smaller. For most purposes the tube can be run at maximum voltage, and since contamination of the target is hardly possible (and would be of little account in any case) it can be run at full power.

For elements below Vanadium, i.e. with excitation energies below 5 keV, the white radiation intensity, from a W tube is rather low and better excitation can be obtained using a Chromium target tube, again at maximum voltage and power. The intense CrK radiation (λ = 2.3Å) will excite atoms of elements from Ti downwards considerably more effectively than the white radiation from a W tube.

Background to Characteristic Peaks

With electron bombardment the background is primarily white radiation from the specimen. This is a major factor in limiting the sensitivity of fluorescence analysis by electron excitation. The ability to subtract this background satisfactorily and directly in the case of energy dispersive analysis is an important advantage, but even so errors inevitably occur in the subtraction process.

With photon excitation the only effective background comes from incident radiation scattered by the specimen. This consists of white and characteristic radiation from the X-ray tube.

This scattered radiation is much less than the excited white radiation background from electron bombardment, but nevertheless should be minimized. It is also necessary to beware of the scattered characteristic lines from the X-ray tube, e.g. W(L) at 1.5 and 1.3Å or Cr (K_α) at 2.3 and Kβ at 2.1Å. In Fig. 10 the WL lines from a tungsten tube have been scattered by a water sample, but might be interpreted as showing the presence of W in the sample. In a sample actually containing W the scattered lines would add to the intensity of the genuine excited lines.

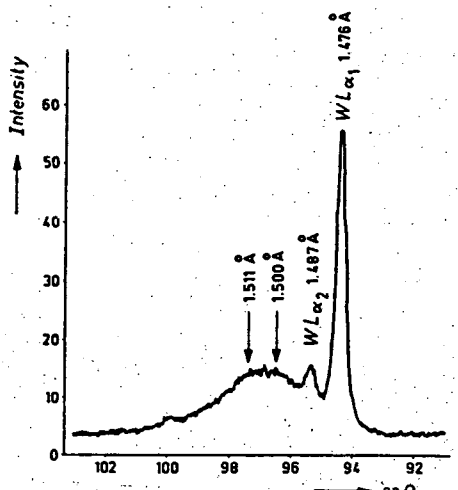

Fig. 10 - The effect of compton scatter on scattered X-ray tube (w) lines. The spectrum of second order $W(L\alpha_1)$ and $W(L\alpha_3)$ was recorded using LiF (200) crystal and a sample of distilled water. The broad compton peak to the long wavelength side of the coherently scattered lines consist of two incoherently scattered maxima each 0.024Å greater than the corresponding coherent line compton shift for a scattering angle of 90°.

Scattered radiation consists of two parts, coherently scattered radiation, which we have been considering up to the present, and incoherently scattered radiation (Compton scattering). The first is scattered without change of wavelength and is polarized. If the scattering angle at the specimen is 90° in a vertical plane, the scattered radiation will be completely polarized in a horizontal plane. If the Bragg reflection from the analyzing crystal is in the horizontal plane, for $2\Theta = 90°$ the coherent scattering will be nearly zero (there will be a range of scattering angles at the specimen, around 90°) and will be reduced at other θ angles.

The second, Compton scattered component has a change of wavelength given by $\Delta\lambda = 0.0243\ (1-\cos\phi)$ Å, where ϕ is the scattering angle. For $\phi = 90°$, $\Delta\lambda = 0.024$ Å. The change in λ is only dependent on the angle of scattering, but since there is a considerable spread of angles in practice, there will be unpolarized white radiation scattered with a change in λ which will be undetectable, and a broadened peak on the long wavelength side of the coherently scattered characteristic line from the X-ray tube. Fig. 10 shows these broadened peaks for WL. The Compton scattering is not reduced by having the planes of scattering and reflection at right angles, and the intensity relative to coherent scattering is strongly dependent on atomic number and scattering angle being much greater for light elements and large ϕ.

Characteristic X-ray generated deep in a light element specimen by an electron beam may suffer Compton scattering so much on the way out to the surface as to produce a significant shift in the peak position. This effect can happen with electron probe micro Analysis (EPMA) and scanning electron microscopy (SEM).

The Compton peak in Fig.10 is resolved from the coherent peak with the wavelength dispersive system (WDS). In energy dispersive systems (EDS), where resolution is much less, it would not be resolved but would distort the peak and slightly shift the position of the maximum.

Characteristic X-rays generated deep in a specimen which contains elements with neighbouring atomic numbers can be altered in relative intensity on the way to the surface. The high energy K radiation from the element of higher Z will be strongly absorbed in exciting atoms of lower which will then produce additional low energy K radiation to add to that originally produced. The enhanced low energy K radiation then emerges with low absorption. This reduction of one component and enhancement of the other (matrix effect) gives rise to errors in fluorescence analysis.

Absorption coefficients

The process of X-ray absorption is almost entirely dependent on the number of atoms of various kinds in the path of the beam. For a monochromatic beam the effect is independent of intensity, i.e. a thickness of material which will reduce the intensity of a strong incident beam to 1/10, will reduce a weak beam to the same fraction. The transmitted intensity I (energy flow rate/unit area) and the incident energy Io are therefore related by an exponential function of the number of atoms of various kinds in unit area of the path of the beam.

$$I/Io = e^{-x} \text{ where } x = \mu^1_a N_1 + \mu^2_a N_2 + \ldots + \qquad (1)$$

μ^r_a is the **atomic absorption coefficient** for the r^{th} atom (which is a constant for a given wavelength) and N_r the number of atoms of type r.

Since what is normally known is the density, d, thickness, t, and elemental composition of the absorber (e.g. the chemical formula), we have, for unit area :

$$td = (N_1W_1 + N_2W_2 + ..)\, m_H$$
$$= (n_1W_1 + n_2W_2 + ..)\, Nm_H = MNm_H$$

where n_r is the number of atoms of type r (atomic wt. W_r) in the known chemical unit, N is the (unknown) number of chemical units, and M is the molecular weight. m_H is the mass of the hydrogen atom.

$$N = td/Mm_H \text{ and } x = td/Mm_H\, \Sigma\mu^r_a\, n_r = \mu t. \qquad -(2)$$

μ is called the **linear absorption coefficient**, and depends on the physical state and composition of the absorber, where μ_a is a constant for a particular element and wavelength.

μ_a is a very small number and it is more convenient to list the gram atomic coefficient $\mu_g = \mu_a/m_H$. - (3)

$$\mu = d/_M\, \Sigma\mu^r_g n_r \qquad -(4)$$

The experimentally determined (or semi-empirically calculated) μ_a or μ_g can be looked up in tables and μ calculated from the chemical formula and d.

It often happens that the elements in an absorber are known as proportions, P_r, by weight.

$$P_r \quad \frac{N_rW_r}{\Sigma NW} \text{ and } (\Sigma NW)m_H = td$$

$$N_r - \frac{td}{m_HW_r}\, P_r$$

$x = td\, \Sigma(\mu_g{}^rP_r/W_r)$ from (1) and (3)

A third absorption coefficient, μ_m is defined as μ_g/W and is called the mass absorption coefficient since tdp_r, its multiplier, is the mass of element r per unit area.

$\mu = d\Sigma\mu^r_m\, P_r$, and this is probably the most useful - (5) formula for calculating the linear absorption coefficient, partly because improved tables of μ_m are more readily available.

The relations between the listed coefficients are therefore :

$$\mu_m = \mu_g\, /W \text{ and } \mu_g = \mu_a/m_H$$

The absorption coefficient for an element varies rapidly with wavelength, and the curve of μ vs ν has discontinuities at the absorption edges. Between absorption edges μ varies approximately as λ^3. Fig.7 shows typical curves.

Absorption coefficients are listed in the International Tables.

Absorption effects are important in X-ray diffraction, since they reduce the diffracted intensities by varying amounts, depending on the geometry of the specimen and its composition. In fluorescence analysis, absorption effects in the matrix can have a considerable effect on the intensity of characteristic X-ray from a particular element in the specimen and, unless allowed for, can cause considerable errors in quantitative analysis.

Dispersion and measurement of characteristic wavelengths

Characteristic photons have

a) Characteristic energies

b) Characteristic wavelengths

— related by $E_{photons} = hc/\lambda$,

Either of these properties (or a combinat l on) can be used to separate out the fluorescent radiations from a mixture of elements (and Kα, Kβ, L, etc. radiations from one element).

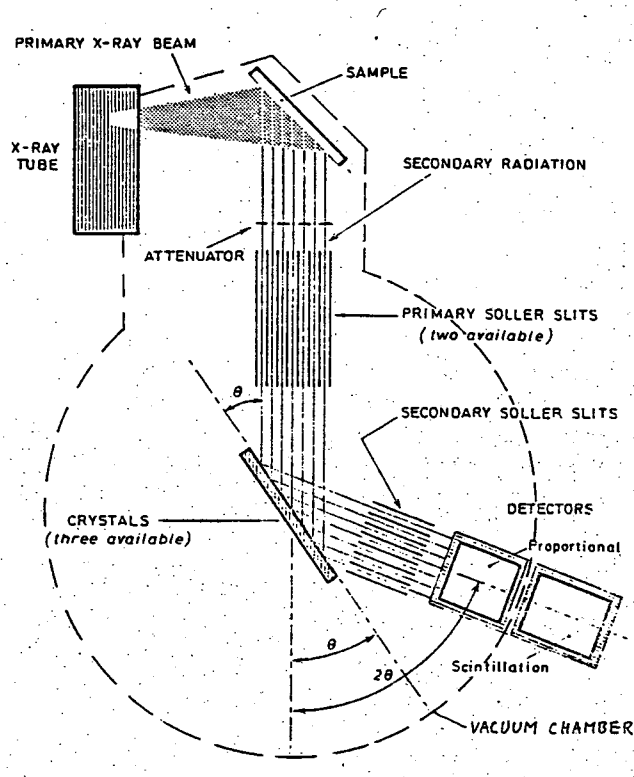

Fig. 11 - Schematic diagram of a Bragg X-ray spectrometer. The X-ray tube and sample have been rotated 90° about the primary Soller slit axis, to bring them into the plane of diagram.

X-ray wavelengths hence their photon energies are measured with a Bragg crystal spectrometer. Parallel X-rays from a collimator falls on a crystal face with Bragg spacing d while a detector is set to receive a reflected beam (Fig.11). Interference of reflections from Bragg planes will give a resultant reflection only if $2d\sin\theta = n\lambda$ is satisfied. Therefore if we observe a reflection then $2d\sin\theta = n\lambda$ is satisfied. n is a positive interger known as order of reflection (n=0 ---> direct beam). If d is known λ can be calculated. During sampling of a mixture of wavelengths the crystal is rotated at a certain speed while the detector in reflected position is rotated at twice the speed. Those wavelengths that satisfy the Bragg relation give peaks (i.e. spectral lines). A Penta erythritol (PE) crystal with d spacing 4.371A° (002 planes) give a first order (n=1) reflection at $2\theta = 109.20$ for Si K_α line (λ = 7.126). However, the fourth order (n=4) Co K_α line (λ = 1.780) also gives a reflection at 2θ = 109.20°. Two different waves reaching the same position can be taken care of by the pulse height analyzer (explained later). Note that the two photons have different energy and energy discrimination is possible with suitable detectors and electronics.

The geometry of the Bragg spectrometer in XRF analysis is similar to that of a powder diffractometer, except that the source is extended -the area of the specimen irradiated by the W tube to excite fluorescent radiation is normally several sq. cm - and careful collimation, especially with the primary Soller slits is essential.

The diffracted beam is broad and also requires collimation with Soller slits. Since long wavelengths may be involved (for MgKα, = 9.9Å) the main X-ray path must be in vacuum (Fig. 11).

Mechanical considerations limit the highest value of 2θ to about 146° (θ = 73°) and values of θ less than 5° are rarely used because the spread due to Soller slit divergence becomes comparable with the resolution, and the analyzing crystal only intercepts part of the beam. $\Delta\lambda/\lambda = 6T\theta \cot \Delta\theta$, and at θ = 5°, is only 1/10th of its value at θ = 45°, for a given θ. If a first order diffraction occurs at too low an angle it is always possible to use the second or higher orders, where dispersion is greater.

For an incident beam width of 12.5 mm and an analyzing crystal 65 mm long the whole of the beam is no longer intercepted by the crystal for θ $\sin^{-1}$ 12.5/65 = 11°. For practical purposes, therefore, θ is restricted to 10-73°. The most generally used crystals are LiF, Pentaerythritol (PE) and Ammonium dihydrogen phosphate (ADP). The table gives details of these crystals and the limitations on their use arising from the minimum and maximum values of θ.

			LiF Lithium Fluoride (200)	PE Pentaerythritol (002)	ADP Ammonium Dihydrogen Phosphate (110)
d			2.014	4.371	5.325
(λMax)			3.83	8.35	10.20
(λMin) (1st order)			0.7	1.5	1.8
Lowest Z &	K		19 (Potassium) 3.74	13 (Aluminium) 8.34(β = 7.98)	12 (Magnesium) 9.89
	L		47 (Silver) 3.70 (β_2)	35 (Bromine) 8.13 (β_1)	32 (germanium) 10.19 (β_1)
Highest Z (1st order)	K		42 (Molyboleum) 0.71	29 (Copper) 1.54	26 (Iron) 1.94
	L		No restrictions	72 (Hafnium) 1.57 (α)	67 (Holmium) 1.85 (α)
nth order - Z	K / —— / L	2	27-58	19-41	17-37
		3	32-70	22-49	20-45
		4	37-79	25-56	23-52
		2	66-	47-	44-92
		3	79-	58-	52-
		4	90-	63-	58-

Table 1. - Limitations for various crystal plates.

Angle between peaks for neighbouring atomic numbers

From Moseley's relation

$\lambda = (Z-\delta)^{-2}$, where K & δ are constants for the transition concerned, and

$\lambda = \frac{2d}{n} \sin\theta$ (Bragg's law),

we have :

$K(Z-\delta)^{-2} = 2d \sin\theta$, $\sin\theta = nK(Z-\delta)^{-2}$

Differentiating (n and d constant) gives :

$-2K(Z-\delta)^{-3} \Delta Z = \frac{2d}{n} \cos\theta \Delta\theta$

$\Delta\theta_1 = \frac{-nK(Z-\delta)^{-3}}{d(1-\sin^2\theta)^{1/2}}$ for $\Delta Z = 1$

$$\Delta\theta_1 = \frac{-nK(Z-\delta)^{-3}}{d\left[1-\frac{n^2K^2}{4d^2(Z-\delta)^4}\right]^{1/2}} = \frac{-2nK}{(Z-\delta)(4d^2(Z-\delta)^4-n^2K^2)^{1/2}}$$

The root in the denominator cannot be less than zero (i.e. $\sin\theta \leq 1$) and decreases if n increases or Z decreases with d constant, or if d decreases with n and Z constant.

Spectrometer Resolution

For n and Z (i.e. λ) constant
$\Delta\theta_1$ increases as d decreases (i.e. θ increases)
For n and d constant,
$\Delta\theta_1$ increases as Z decreases (i.e. λ and θ increase)
For d and Z constant,
$\Delta\theta_1$ increases as n increase.

Use the crystal with smallest possible d and increase n to increase resolution.

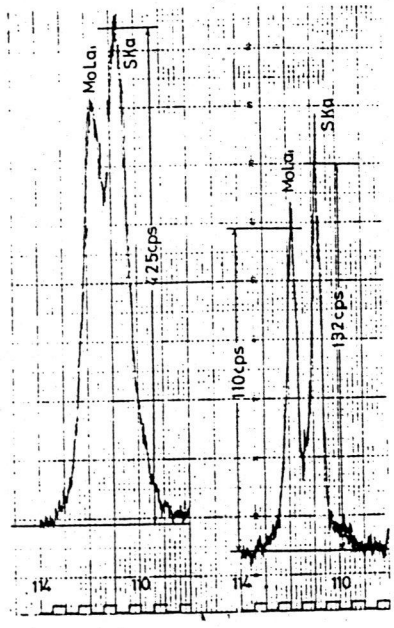

Soller slit 0.4° Soller slit 0.1°
Full scale 500 cps Fulls scale 200 cps

Fig. 12 shows the peak profiles of Mn Kα and CrKβ (same reflection order n) from stainless steel. If Topaz is used as the analyzer crystal the separation will be twice as that with a crystal of LiF.

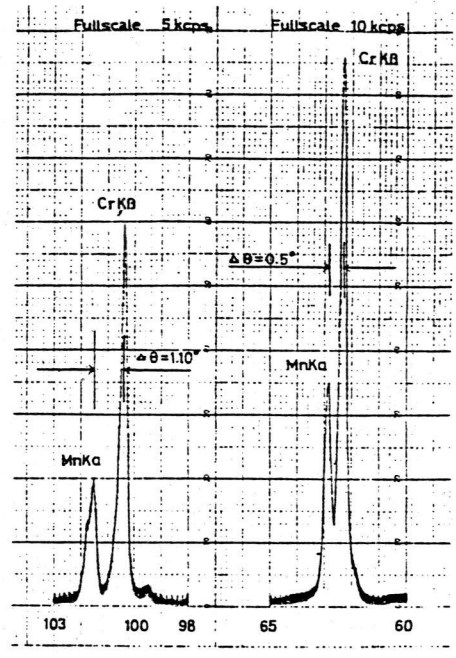

Separation of SKα and MoLα in stainless steel (with parallel beam method fluorescent X-ray analyzer)

Fig.13 - Separation of MnKα and CrKβ by LiF and Topaz.

Effect of soller slits in resolution

Soller slit is made by arranging thin plates of heavy metal such as molybdenum, leaving appropriate space in between each plate (Fig.11). This is used in order to extract parallel X-rays. For both focusing method and parallel beam method of analyzer, the X-ray intensity decreases if resolution is increased by narrowing the soller slits. Narrow slits make nearly by peaks 'not' to enter the detector. The energy separation between such peaks can be low that they cannot be separated by PHA alone. Therefore, in heavy element region where peaks are close to each other, resolution should be increased at the sacrifice of the X-ray intensity. For the light element region where the X-ray intensity is low, slit width should be expanded so that the X-ray intensity will be raised at the sacrifice of resolution.

Fig.13 shows one of such examples. When analyzing S in the stainless steel, MoLα, peak appears near SK_α, if germanium is used as the spectral crystal. In order to eliminate any effect of MoL α, it is necessary to use a solar slit with a high resolution as shown in this figure. (If NaCl is used as the spectral crystal, the peak separation will

be more than twice compared with the case where germanium is used. Thus, the effect of MoL α, can be eliminated easily. However, NaCl cannot be used for P. (The secondary reflection appears).

Detectors

Originally Geiger counters were used in which photons merely triggered a standard height electrical pulse. **No energy discrimination was possible and only angle** dispersion. Therefore peaks of all orders occurred on the diffraction trace of I v.s 2θ and a great deal of over-lapping was liable to occur.

Gas proportional counters (flow and sealed) and scintillation counters give pulses proportional to the energies of the photons, but with a spread of pulse heights due to the variations in the ionization processes in the counter. This spread reduces the discrimination possible by using an electronic 'gate', which allows through only those pulses lying between two set voltage levels. However, photons from orders other than that being measured can be suppressed, so that there is far less over-lapping of peaks. If a proportional detector with sufficient resolution could be made, the crystal analyzer could be dispensed with and a trace obtained of intensity against energy by moving the height of a very narrow window. The peaks would then correspond to characteristic fluorescent radiation, in terms of eV instead of 2θ. Energy dispersion system (EDS) with considerable improvement on the electronic side but less resolution than a crystal spectrometer is now available. NB such solid state detectors need to be kept in liquid nitrogen at all times to avoid deterioration and destruction.

Gas flow proportional and scintillation counters

In the conventional spectrometer these are mounted in tandem (Fig.11), the proportional counter inside the vacuum chamber (with gas flow to minimize the effect of leaks) and the scintillation counter outside. Any photons which go through the proportional counter and the vacuum chamber window are incident on the scintillation counter, which has nearly 100% efficiency until the protective and light tight window starts to absorb significantly between 2-3Å. The flow proportional counter with Ar/CH_4 filling absorbs over 75% of photons at 3Å and its efficiency, apart from a dip at 4Å due to the absorption edge of Ar, continues high until the 6 micron mylar window begins to absorb heavily at 9 - 10Å.

The pulses from the two counters must be adjusted to the same height before being mixed and fed to the single channel pulse height analyzer. The pulse heights can be adjusted equal by coarse adjustments, if necessary, on the preamplifiers, and fine adjustments to the individual E.H.T. supplies to the counters.

Pulse Height Analysis

To determine the spread of pulse heights and the maximum of the distribution for a given wavelength (e.g. CuKα) put a specimen containing copper in the holder and set the spectrometer angle to correspond to the 2θ angle for 1.39 . Make slight angular adjustments to obtain the maximum reading on the ratemeter. The two counters should be checked separately if (a) the purpose is to check the functioning of the counters, or (b) they have separate single channel analyzers, which can be set individually (the spread of pulses from the Gas flow counter is much less than from the scintillation counter) or (c) if the positions of the maxima of the pulse height distribution curves are to be adjusted equal and at the correct height for automatic pulse height analysis (q.v.) while scanning. If the counters are known to be functioning properly and to give equal pulses which are mixed and fed to one single channel analyzer, then the distribution curve need only be done once for the two counters together, as a means of setting the window limits.

With the spectrometer 2θ angle fixed on the line to be measured, a narrow window (approximately 1/10 of the pulse height for CuKβ) is set and the low level adjusted just above the noise level. The ratemeter reading is noted. The low level is then moved up by a step approximately equal to the window width, and the new reading noted. The intensity (i.e. counts or ratemeter reading for each position) is plotted against the pulse height (i.e. the mean window position which equals the low level + half window width) and the full width of the peak in the curve is measured at half maximum height (FWHM) to find the resolution. The top and bottom of the gate are set where the curve levels out on either side of the peak (A and B, Fig.14).

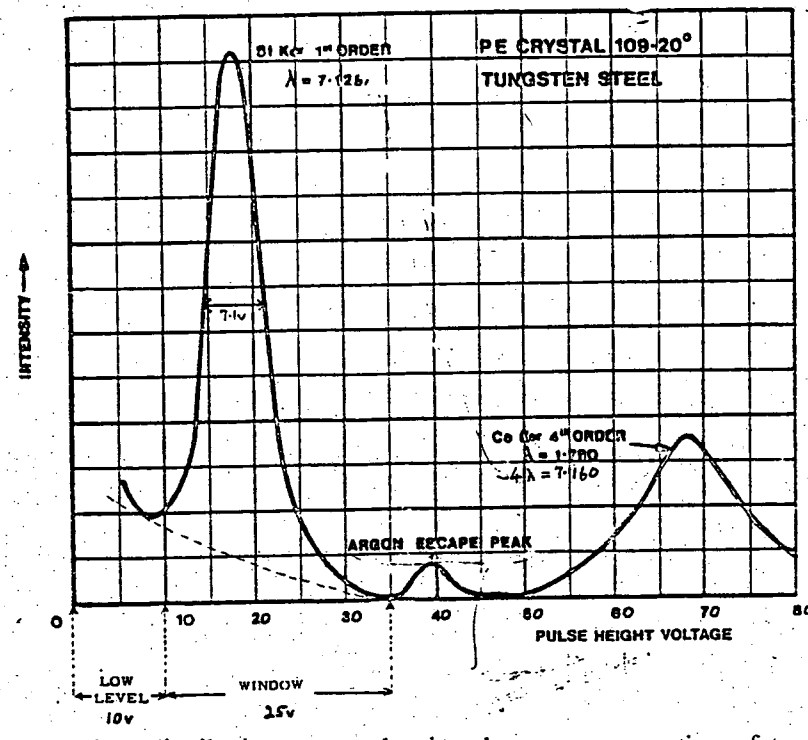

Fig.14 - Pulse height distribution curve, showing the energy separation of two peaks which overlap on the spectrometer recording (Fig.15).

Fig.14 shows the curve for a specimen containing Si and Co. The 1st order Si Kα peak overlaps the 4th order Co Kα to some extent, so that some Co Kα photons are reflected when the spectrometer is set on the Si Kα peak. These have four times the energy of the Si Kα photons and produce the high voltage peak shown in the Figure. If the window is set from 10 to 35 volts all the Co Kα photon pulses will be rejected. (Window values vary from machine to machine depending on electronics).

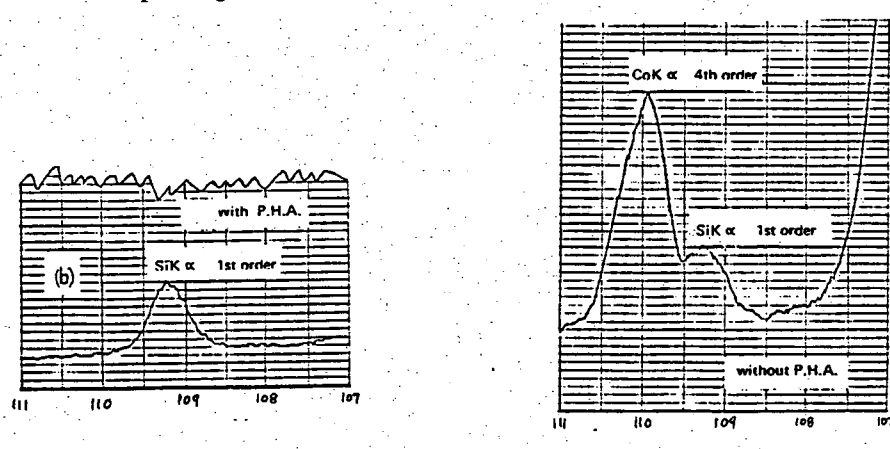

Fig.15(a) - A recorder trace of a spectrometer scan over the SiKα wavelength (i.e. changing θ and 2θ). Without pulse height analysis the high background partly due to FeKβ at 106°) and interference from CoKα tends to swamp the analytical line.(b) - The same scan with pulse height analysis in operation. The background has been reduced (partly by eliminating FeKβ) and the interference from CoKα fourth order, on Si, Kα first order, has been completely eliminated.

Fig.15(a) shows a spectrometer trace (i.e. varying θ , 2θ) of the specimen, obtained without pulse height analysis. (A geiger counter would give this trace, with no possibility of separating the peaks). Fig.15(b) is the trace obtained after setting the pulse height window as above. Only the Si Kα peak is present, without the slight shift in position produced in (a) by the presence of the Co peak.

When an automatic scan over the whole range is required the photon energy (and therefore the counter pulse height) is continuously varying. The window height must also be varied correspondingly (or PHA abandoned) and this can be provided by means of a potentiometer moved by the spectrometer arm.

The peak width

In Fig.14 the full width at half maximum (FWHM) of the Si Kα peak is 7.1v. The pulse height of the peak maximum, V = 17.5v. The resolution, R = W/V = 40% for = 7.126Å. Before we can compare this with standard resolutions is must be converted into the value for a standard wavelength. R is a function of the number of ion pairs produced by a single photon. The process is a random one and if the average number of ion paris is n, the standard deviation will be $\sqrt{n}$, if the distribution is a Gaussian one, which can in fact be shown to be a good approximation. For a Gaussian curve,

$R = 2.36\sqrt{} = 2.36\ (\sqrt{n}/n) \times 100$. For Argon, the average energy required to produce an electron pair is 26.4 eV.

$n = E/0.0264$ where E is the photon energy in keV.

$R = 38.3\ /\sqrt{E}$ since $E = K/\lambda$ $R1/R2 = \ldots \lambda_1/\lambda_2$

The scintillation counter requires much more energy to produce an effective blue photon and the resolution is much worse. R = 129/ E. Otherwise the analysis is the same.

If we now use above equation to convert the resolution for Si Kα to that for Fe Kα (λ = 1.937Å), which is usually used as a standard, we have :

$$R(Fe) = R(Si)\ \frac{1.937}{7.126} = 40 \times 0.52 = 21\%$$

This is larger than the theoretical 15% and indicates that the proportional counter (which absorbs all the Si Kα photons) is not in perfect condition. However, a deterioration to 25 - 30% can be tolerated before the counter requires reconditioning. The scintillation counter should not be much worse than 70% for Fe Kα. If it is, the phosphor crystal probably wants replacing.

The Argon Escape Peak

The small peak in Fig.14 is due to a particular aspect of the ionization process in a gas proportional counter. Most photons produce a number of ion pairs by interaction with the **outer electrons** of the Argon atoms, the number of pairs being proportional (with statistical fluctuations) to the energy of the photon. But occasionally part of the photon energy is used to eject a K electron and the remainder then produces correspondingly less ion pairs. If the K ionized atom decays by producing an Auger electron, this will generate the missing ion pairs, and since the decay time is very short, a normal pulse will be produced. If an Ar Kα photon is produced and absorbed inside the counter the same thing will apply. But all elements have a low absorption for their own characteristic photon is just less than that required to eject an electron from the corresponding level (K in the case of Argon) and this absorption mechanism is therefore not available. The wavelength is thus just on the long side of the absorption edge, where the linear absorption coefficient is very low. Some of the Ar Kα photons therefore 'escape' from the counter (actually they are absorbed in the walls, but do not produce any ion pairs in the gas). The pulse produced in this case is smaller than it should be, because the ion pairs corresponding to the energy of an Ar K photon have not been produced. The pulse, in other words, corresponds to a photon whose energy is that much less, and on the pulse height distribution curve it will produce an 'escape peak'. It really should be called a 'remainder peak', since it corresponds to the remainder of the energy, left when the Ar Kα photon 'escapes'.

The position of the escape peak is very easily found. Since the peak voltage, $V = K/\nu$ (i.e. is proportional to the photon energy and therefore to the frequency), we have from Fig.14, $V_{Co\ K\alpha} = 68 = K/1.791$

$K = 68 \times 1.791$. $V_{Ar\ K\alpha} = 68 \times 1.791/4.192$ ($\lambda ArK\alpha = 4.192Å$)

$V_{ESC} = V_{CoK\alpha} - V_{ArK\alpha} = 68(1-1.791/4.192) = 39V$

Since the escape peak depends on the K ionization of Ar (absorption edge 3.871Å) only photons more energetic than this (i.e. shorter wavelength) can produce an escape peak. Also, the further the incident wavelength is away from the absorption edge, the smaller the proportion of K ionizations of Argon becomes (see Fig.6). Also, since the energy shift is constant, it becomes a smaller proportion of the main peak height and as the main peak width, W

is proportional to V, increases with the pulse height, the escape peak not only becomes smaller, it ceases to be resolved and is counted with the main peak. The elements affected significantly are from K (19) to Co (27). The escape peak for K, being the difference between two nearly equal energies (ArKα & K Kα) is of such low energy that it is lost in the noise. For Ca to Co a decision has to be made whether to include the escape peak when setting the analyzer window, or to exclude it at the cost of losing 5 - 10% of the counts. Since to include it, at least up to Co (27) means including considerably more background it is usually better to set the window round the main peak, and exclude the escape peak.

Energy Dispersion

Solid state silicon detectors, developed originally for radioactive counting, can now be used for X-ray detection. The X-ray photon produces a large number of photo electrons in the silicon, which interact with the silicon atoms to raise bound electrons to the conduction band. Each such event requires 3.8eV of energy (c.f. the ionizing energy for Ar of 26.4eV). The total energy of the photon is converted (with statistical variations) into free electrons and the total charge, collected by an applied bias voltage in less than 1μs, is therefore proportional to the photon energy. In order to prevent loss of electrons during the collection process it is necessary to fill up any imperfections or dislocations in the silicon lattice, which would trap electrons. This is done by diffusing in lithium atoms.

In order to obtain the resolution implied in the very low 3.8eV energy per conduction electron it is necessary to reduce interfering thermal effects, both in the detector and in the field effect transistor (FET) preamplifier. Both must be cooled to liquid nitrogen temperatures, and this is a considerable limitation on energy dispersion systems. Their great advantage is in systems where only low intensity from a localized source of X-rays occurs. The detector can be placed close to the source so that a large collection solid angle is achieved. The position of the source is not nearly so critical as in wavelength dispersion. It is particularly suitable for SEM work.

The preamplifier produces a step output, the height of each step being proportional to the absorbed photon energy (Fig.16). The amplifier produces pulses whose heights are proportional to the steps, and each pulse charges up a capacitor, which is then discharged at constant current. The time taken to discharge is converted to the address of the corresponding channel of an 800-1000 channel pulse height analyzer. This channel registers and stores the count. The photons are thus registered in the channels corresponding to their energies. The total count in each channel can be displayed on a CRT.

A further advantage of the drifted silicon detector is that it is nearly 100% efficient over a wide range of energies (and therefore wavelengths). Fig.17 shows this wide range from Na to Ag or higher for K photons.

The whole spectrum is collected at the same time and a small computer can be used to manipulate the spectrum in various ways and produce integrated peak counts for selected peaks. These can then be used in the same way as the integrated counts from a wavelength dispersive spectrometer.

The resolution is considerably less than for wavelength dispersion - about 150eV at 6keV compared with 10eV for LiF (200). However, it is adequate for separating Ka peaks from neighbouring elements and overlapping peaks from different elements such as Skα and Pb Mα, or K$\beta$and Kα peaks from some neighbouring elements such as Ti Kβ and VKα can be dealt with by 'stripping' one peak electronically. Similarly, background stripping can be done by the same small computer.

The electronic equipment are expensive and the silicon detector must be kept continuously cooled with liquid nitrogen, even when not in use for long periods. It remains to be seen how far the new system will displace wavelength dispersion with partial energy discrimination.

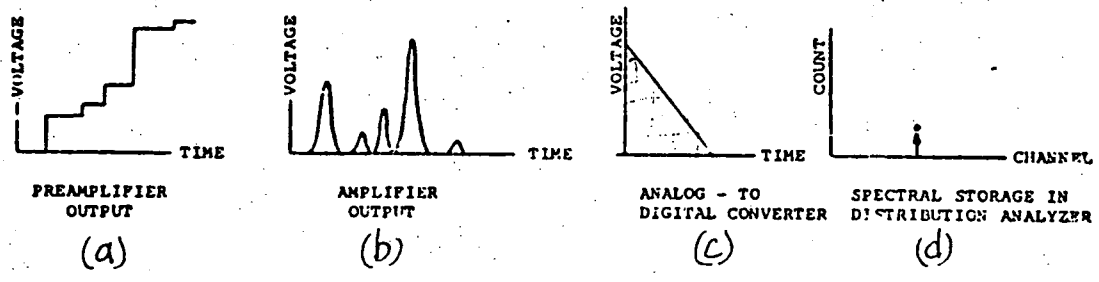

Fig.16 - Stages in the production of an Energy Dispersive Spectrum.

a) The stepped voltage output from the FET preamplifier. Each step corresponds in height to the energy of a photon registered by the detector. The FET is discharged at intervals and the lost time automatically allowed for in the circuitry.

b) Each preamplifier step is turned into a pulse, whose height is proportional to the step height.

c) Each pulse charges a condenser, which discharges through a constant current circuit. The time of discharge, which is proportional to the pulse height, is turned into the address of a particular channel in the multichannel analyzer.

d) This channel registers and accumulates the count.

These steps occupy a microsecond or so, and the spectrum builds up in the multichannel analyzer and is displayed on a CRT.

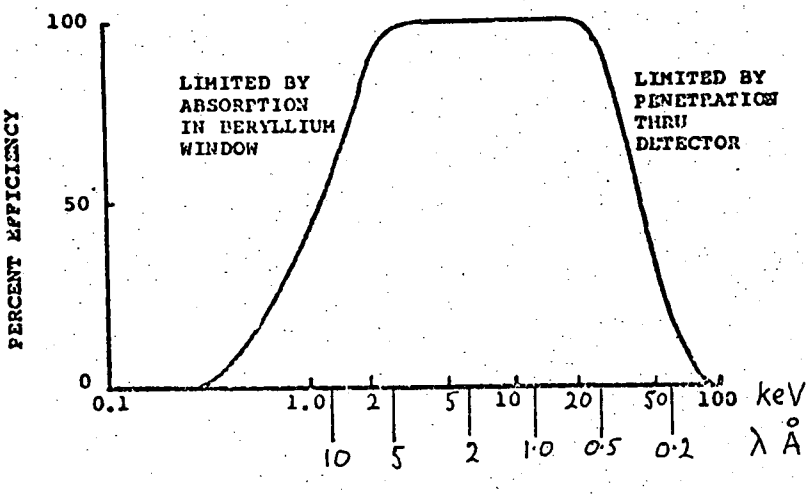

Fig.17 - Spectral response of Lithium drifted silicon detector

Errors due to statistical fluctuations in the Count Rate

The production and absorption of X-rays is subject to random fluctuations, so that the numbers of counts recorded in equal times (other conditions remaining constant) have a Poisson distribution, similar to that found for radioactive disintegrations. One can replace the very small probability of a radioactive atom disintegrating, by the correspondingly small probability of an atom in the target material being excited and producing a characteristic

photon which is absorbed in the counter. In both cases the assumption is that the number of atoms is very large and in the second that the number of bombarding electrons or photons is also very large. The binomial distribution, with probability p that a particular event will occur, and q = 1-p that it will not, which was developed in the theory of tossing coins or rolling dice, is modified in the Poisson distribution by assuming that n, the number of 'trials' gets definitely large and p, the probability of any one 'trial' producing the specified result gets indefinitely small, but in such a way that the product, np remains finite, so that there is an 'expectation value ; μ = n p, of the result of the large number of trials. In our case there is an 'expectation value' of the number of photons registered by the counter in a specified time, say one second. An approximation to this 'expectation value' is obtained by registering the number of counts, N_r, received in a large number of second intervals and taking the average, $\bar{N}$. The distribution of the values of N_r can also be plotted and shown to correspond to a Poisson distribution.

The standard deviation, σ, of the binomial distribution can be calculated and is equal to $\sqrt{npq}$. In the Poisson distribution np = μ and q = 1-p --> 1 $\therefore \sigma = \sqrt{\mu}$.

In any given observation, the number of counts, N, registered is an approximation to the 'expectation value'; μ. $\sqrt{N}$ is therefore an approximation to the value of σ. The larger N is, the better the two approximations become. The following table gives some idea of the possible effects of the approximation. N' is a single observation, $\sigma = \sqrt{N'}$ is the approximation to the standard deviation. The assumption is then made that by an unlucky chance, this value is less than the 'true' or 'expectation' value by 3σ (this chance is about 1 in 1000). The 'true' values N and $\sigma = \sqrt{N}$ are calculated on this assumption and the next column gives σ'/σ as a percentage. Finally, the coefficients of variation $\sigma(N')/N' = \sqrt{N'}/N' = 1/\sqrt{N'}$ and

$\sigma(N)/N = 1/\sqrt{N}$, which (x 100) are a measure of the 'percentage error' due to counting statistics, are also given.

N	$\sigma' = \sqrt{N'}$	N	$\sigma = \sqrt{N}$	σ'/σ%	$\sigma(N')/N' = 1/\sqrt{N'}$%	$\sigma(N')/N = 1/\sqrt{N'}$%
4	2	16	4	50	50	25
9	3	24	4.9	62	33	20.5
16	4	33	5.8	69	25	17.3
25	5	45	6.7	74	20	14.9
400	20	465	21.6	92.6	5	4.6
10,000	100	10,305	101.5	98.5	1	0.99

It is clear that great care has to be taken in interpreting the meaning of small numbers of counts, but that in the 10,000 region and above, a single observation will give an accurate value of $\sigma(N)$.

For large values of N, the Poisson distribution approximates to a normal distribution and we can use the properties of a normal distribution to say that the 'true value lies in the region N $\pm \sqrt{N}$ with a 68% probability; in N $\pm$ 2$\sqrt{N}$ with a 95% probability; and in N $\pm$ 3$\sqrt{N}$ with a 99.73% probability. For N = 10,000 this means that only in less than 3 in 1,000 trials should the recorded count lie outside 9,700 - 10,300. More strictly, if the average N of a 1,000 trials is 10,000 less than 3 counts should lie outside this range.

For the purposes of estimating the errors in fluorescence analysis it is generally sufficient to remember that the standard deviation of N counts is $\sqrt{N}$. Since it is the count rate R that is normally measured, then if N counts are measured in T seconds, R = N/T and $\sigma(R) = \sqrt{N}/T$.

Usually the timing error is so small that it can be neglected, but if the analytical count is made during the accumulation of a preset number of monitor counts, then there are two independent errors. Let M be the monitor count and N the analytical count.

The monitor is measuring an effective time which corrects for fluctuations in output of the X-ray tube. However, this time has a standard deviation due to the statistical variation in the count M.

$\sigma(T)/T = \sigma(M)/M = 1/\sqrt{M}$, $\sigma(N)$ is due to the random variations in the counting process and equals $\sqrt{N}$. But

there is an additional independent error in N arising from $\sigma(T)$, given by
$N/T\ \sigma(T) = N/\sqrt{M}$. Therefore the combined standard deviation :

$$\sigma(N_c) = \left[(\sqrt{N})^2 + \left(\frac{N}{\sqrt{M}}\right)^2\right]^{1/2} = N\left(\frac{1}{N} + \frac{1}{M}\right)^{1/2}$$

The monitor counts should therefore be as large as possible to reduce the total error in the analytical count. If M = 2N, the total error is only 20% more than that due to $\sigma(N)$ alone, but if M = ½N, the total error is over 70% more.

A similar effect occurs in subtracting a background measurement from a peak measurement to get the true peak height. Let P be the peak count, accumulated over T_P seconds, and B the background count over T_B secs.

$R_p = P/T_p$; $R_B = B/T_B$: $R = R_p - R_B$;

and, since the errors of R_p and R_B are independent,

$$\sigma(R) = (\sigma^2(R_p) + \sigma^2(R_B))^{1/2}$$

$$\sigma(R_p) = \sigma(P)/T_p = \sqrt{P}/T_p; \quad \sigma(R_B) = \sqrt{B}/T_B$$

$$\sigma(R) = (P/T_p^2 + B/T_B^2)^{1/2}$$

The second term should be kept to 50% or less of the first, but this normally means that the time spent in background counting need only be half or less of that for the peak.

There are three main ways in which counting can be carried out :

a) Fixed Count. $R_pT_p = R_BT_B = N$. The times are recorded and $R_p = N/T_p$, $R_B = N/T_B$. Total time $T = T_p + T_B$.

b) Fixed time $N_P = R_PT/2$, $N_B = R_BT/2$
$R_P = 2N_P/T$, $R_B = 2N_B/T$

c) Fixed Time Optimal $T_P/T_B = R_P/R_B$; $T = T_P + T_B$
The times, $T_P = \frac{T\,R_P}{R_P + R_B}$ $T_B = \frac{T\,R_B}{R_P + R_B}$

are calculated from approximate values of R_P and R_B, the counts N_P and N_B recorded for these times and $R_P = N_P/T_P$, $R_B = N_B/T_B$.

It can be shown that for the same total time T, $\sigma(R)$ is least for (c) F.T.O. and greatest for (a) F.C. Since (c) requires at least a preliminary approximate peak and background count to determine the T_P/T_B ratio for calculating the times for the full count, it is not usually used for a series of determinations of different peaks. (b) F.T. has the advantage of enabling the timing to be controlled and is also more accurate than (a) F.C., so it is normally the method of choice.

In delaying with problems of the standard deviation of a function of several variables, there are two formulae worth memorizing, which can be derived from the general partial differential formula.

If $G = \Sigma a_iM_i$ where M_i are variables with standard deviations σ_i, then

$$\sigma_G^2 = \Sigma a_i^2\sigma_i^2$$

In particular if $G = A \pm B$, $\sigma_G^2 = \sigma_A^2 + \sigma_B^2$

If $G = K\,M^a_1M^b_2M^c_3 \ldots$ where K is constant and a,b,c, exponents,

$$\left(\frac{\sigma_G}{G}\right)^2 = \left(\frac{a\sigma_1}{M_1}\right)^2 + \left(\frac{b\sigma_2}{M_2}\right)^2 + \left(\frac{c\sigma_3}{M_3}\right)^2 +$$

In other words, for a sum of difference one adds the variances (σ^2) multiplied by the squares of the constant coefficients, and for products one adds the squares of the fractional errors (or coefficients of variation).

Sample Preparation

Introduction

Since the fluorescent X-ray analysis method is not absolute but a comparative analysis, specimens to be analyzed must be arranged completely in the same conditions as standard specimens which are compared with. When solid specimens are used, their surfaces must be ground, and when powder specimens are used, their density must be 'equalized'.

Solid Specimens

1) Steel

It is recommended to finish the surface of a steel specimen with emery or a grinder of #80 ~ #100. Although it is better that a measuring surface is smoother, if its surface roughness is of #80 or more, it does not affect measurement accuracy. Furthermore, the effect of the grinding direction by endless paper also can be ignored by specimen rotary mechanism (spinner). When analyzing microcomponents, even a very fine remainder of abrasives has a substantial effect on measured values. When analyzing Al, use an abrasive made from silicon carbide, and when analyzing Si, use one made from alumina. When analyzing a cast iron specimen, it must be turned into white pig iron.

2) Al and Cu Alloys

Since the hardness of these alloys are low, if an emery abrasive is used for finishing their surfaces, it bores into them. It is recommended to use a lathe for finishing. However, when using specimens including plenty of Pb, it may melts over their surfaces due to the heat in machining and have an effect on measured values. Take note of it.

3) Other Specimens

A considerably wide specimen surface is required for the fluorescent X-ray analysis. Usually, an area of ≈ 30 mm^2 is needed and specimens are desired in a plate or ingot shape. If these specimen shapes cannot be obtained, measures should be taken in accordance with each specimen shape. When analyzing a small specimen which does not have a flat measuring surface of ≈ 30 mm diameter, mask the specimen to equalize the size of its measuring surface. In order to materialize this, it is recommended to use a specimen vessel enabling a mask change. However, if a masking method is employed, the fluorescent X-ray of masking material is generated in a large amount and gives a low S/N ratio.

In XRF analysis, it is hardly necessary to take the thickness of the specimen into consideration. The limit of thickness for most of specimens and elements to be analyzed is 10 ~ 100 μ. However, when analyzing specimens consisting of small atomic number elements such as high-molecular specimens, adequate attention must be paid to the thickness of specimens because the X-ray is transmitted through deep thickness. Usually, set the thickness of specimens to 2 mm or more, and when using films, determine the number of them to be piled in advance.

Powder Specimens

1) Pulverization

The grain size of powder specimens has an effect on the fluorescent X-ray intensity. If specimens are sufficiently pulverized, their pressure molding can be easily done. The grain size of specimens generally required is of 300 mesh or more, and their grain diameter is 40 μ or less. If the grain size is coarse, the fluorescent intensity decreases same as in the case of the coarse surface of a solid specimen. A vibrating mill is usually used for pulverizing specimens. However, if they are pulverized for a long time, they are contaminated by the metal of the pulverization vessel. Even though a vessel made from tungsten carbide is used, the specimens are contaminated by Ti, Co in addition to W. If a wet pulverization method is employed by putting a solvent with high volatility (a

small amount of n-hexane, alcohol, etc.) in the pulverization vessel together with a powder specimen upon pulverization, it reduces contamination, improves the effects of pulverization and mixture, and also facilitates the cleaning of the pulverization vessel. When a dry pulverization method is employed, the cleaning of the vessel can be facilitated by pulverizing glass.

2) Pressure Molding

Mold a pulverized specimen by pressure in a specially designed press. This will harden the specimen and prevent it from scattering durng measurement. Also, molding the specimen with a constant pressure standardizes the density of the specimen. Use an Al ring of diameter $\approx$35 mm place it on a flat bed press head, fill it with a powder specimen and press the ring and specimen simultaneously. Use a full pressure of 20 ~ 30 tons. Although the density of a powder specimen molded by a pressure has an effect on the fluorescent X-ray intensity, if it is pressed by a pressure of 15 tons or more, the fluorescent X-ray intensity reaches almost a constant value. Abrupt pressurization or reduction may cause a specimen to crack.

If a specimen cannot be properly molded by applying a pressure of 30 tons, use a binder. Recommendable binder materials are starch, stearic acid, cellulose and styrene maleic acid. Mix one of these materials with the specimen at a 10 - 20% in terms of weight. The binder can be equally mixed in the wet pulverization method using n-hexane.

3) Other Specimens

When the amount of a specimen is too small to fill the Al ring, it is recommended to sprinkle it over an adhesive tape, dilute with a binder or sprinkle it over the binder and mold by a pressure. In this case, be sure to carry out a blank test to check what kinds of elements are contained in a base material in advance.

Liquid Specimens

Liquid specimens are placed on a teflon specimen vessel. A mylar film with o-rings enclose the liquid. They are held together by metal fittings. When measuring in vacuum, use a mylar film with its thickness of 12 μ, and when measuring in the air, use that of 6 or 12 μ. After filling the liquid specimen, put the specimen vessel in a vacuum desiccator and evacuate it. Analyze the specimen after checking that the mylar film is not broken.

An air chamber is provided for the liquid specimen vessel to prevent bubbles from being caused when measuring the specimen in vacuum. If the liquid specimen vessel is placed in the vacuum, the mylar film expands by being pulled (even if the mylar film is held with a mesh or a thick mylar film is used). And as a result, the volume of the liquid specimen vessel expands and its internal pressure is reduced. Due to the pressure reduction, large bubbles are caused by the vaporization of a part of the liquid or gases dissolved in the liquid. In a top-irradiating-type device, these bubbles gather on a measuring surface and the level of a specimen surface changes greatly. Consequently, it may cause an error to a measured value. A specially designed air chamber is provided to prevent it. In this specimen vessel, as the mylar film expands, the pressure of the air chamber changes accordingly. Since the pressure on the specimen liquid is not reduced, bubbles are not caused. (However, very fine bubbles are caused on the inner wall by the irradiation of the X-ray and are stuck there).

Although the mylar film used for the liquid specimen vessel has a sufficient mechanical strength even though it is thin, it may be softened and expands due to the heat generated by the X-ray irradiation. Consequently, it is required to use a relatively thick mylar film (for example, 12 μ thick) when measuring in the vacuum. If a thick mylar film is used, the absorption of long wavelength against the X-ray increases, and the measurement effect in the vacuum decreases by half. Accordingly, when measuring light elements in the liquid specimen, use a mylar film with a thickness of 4 - 6μ (occasionally an expanded polypropylene film with a thickness of approx. 1 μ) to prevent the absorption of the X-ray and measure in the atmosphere of He gas. When measuring in the He gas atmosphere, a thin film can be used.

Enrichment Method

These methods are available for enriching liquid specimens.

a. Filter paper method
Drop a liquid specimen of 0.5 ml ~ 1 ml on a circular filter paper, specially made for the purpose. After drying it, set them to a specimen holder, and measure.

b. Ion Exchange resin method
Adsorb metallic components in a liquid specimen to an ion exchange resin, and dry it for measurement. The dried ion exchange resin cannot be hardened even by pressing. Adhere it to an adhesive tape or put it in a shallow plate-shaped specimen vessel, and cover with a mylar film to prevent scattering.

c. Electrodeposition method
Electrodeposit a metallic component in the liquid specimen on a metal with high purity and measure it. When many components coexist, take note that they are selectively electrodeposited in sequence of a lower decomposition potential.

d. Precipitation enrichment method
Produce a chelate and make it precipitated on a filter paper, and dry it for measurement. Many elements can be enriched simultaneously.

These methods considerably improve measuring sensitivity by enriching the specimen.

Qualitative Analysis

When carrying out a qualitative analysis, sample preparation measuring conditions are not strictly required. The main objective is to identify the elements present. However, when trace elements are searched special considerations may be needed in sample preparation eg. (enrichment, reducing background and interference). These have been discussed earlier.

Having obtained the (intensity) I vs 2θ chart, read off the 2θ angle(s) for the required peak (element).

eg. crystal LiF (200) a peak angle is observed at $2\theta = 45.0°$.

According to standard tables (2) this could correspond to CuKα (n=1). Therefore Cu can be in the specimen. However, the table indicates other possible elements.

LiF	E	B	L	N	Z	LAMBDA	RI
44.96	Ba	K	α1	4	56	1.540	100
44.96	Pa	L	β4	2	91	1.540	20
44.96	Cu	K	α1	1	29	1.540	100
44.99	Ir	L	l	1	77	1.541	30
45.02	Cu	K	α	1	29	1.542	150
45.08	Eu	L	4	1	63	1.544	10
45.08	Cu	K	α2	1	29	1.544	50
45.08	Tu	L	β4	1	69	1.544	20
45.11	Sm	K	α1	5	62	1.545	100

Table 2 - List of Angles (2θ -> Element)

The exact element can be identified by a consideration of the following procedures.

1) The peak of each series does not appear independently.
Kα and Kβ, Lαl, and Lβ1 etc. make a combination and appear with a constant relative intensity ratio (Table 3).

	K Series			L Series	
	Light element	Intermediate element	Heavy element		
Kα1	100	100	100	Lα1	100
Kα2	50	50	54	Lβ1	50
Kβ1	15	21	26	Lβ2	20
Kβ3	0.1	3	9	Lα2	11
				L1	10
				Lβ3	6
				Lβ4	4
				Ll	3
				L3	2
				L2	1
				Ln	1
				Lβ6	6

Table 3 - Relative Intensity of Characteristic X-ray

A pulse height analyzer is normally set to eliminate the higher order reflections (n=2,3). But the presence of higher orders can be searched (for example by widening a window and conducting a PHA). The relation between the reflection order and intensity is approximately as shown in Table 4.

n	Relative Intensity
1 : 2 : 3 : 4 ≈	100 : 20 : 7 : 3

Table 4 - Reflection Order and Relative Intensity

Note that as the Kαl and Kα2 of one element usually appear super-imposed on each other, they are expressed by "Kα". However, peak angle separation increases in higher order reflections, and peaks appear separately (resolved).

Elements are not mistaken by reading two or more peaks per each element and identifying it.

Precautions during scanning
2. Acceleration Voltage
The characteristic X-ray is not irradiated unless the acceleration voltage of an X-ray tube exceeds the excitation voltage of the very element. If the maximum acceleration voltage of the X-ray tube used for the Fluorescent X-ray Analyzer is 50kV, the X-ray of the K series is excited approx. as far as 58 Ce (K series excitation voltage 40,4 kV). For heavier elements, the X-ray of the L series is to be measured.

3. Scattering of Primary X-ray
The primary X-ray may be scattered by a specimen and appear in the spectrum of the fluorescent X-ray. Usually, this is the characteristic X-ray of the anti-cathode substance of the X-ray tube. If a Rh tube is used for example, RhKα, Kβ, CuKα and so on appear.

As the primary X-ray is scattered in proportion to $\frac{1}{Z^{2-3}}$ scattered

X-ray background becomes high in case of water and light molecules.

Quantitative Analysis

Introduction

The basis of XRF quantitative analysis is to use the intensity of one of the characteristic lines of the element and then use this line intensity (I_p) to estimate the concentration (c) of that element. By use of a range of standard materials a calibration curve can be constructed (Fig. 18).

$$y = mx + K \rightarrow I_p = mc + I_B$$
$$c = (I_p - I_B)/m$$
$$C_{unKn} = \frac{(I_p)un - (I_B)un}{m}$$

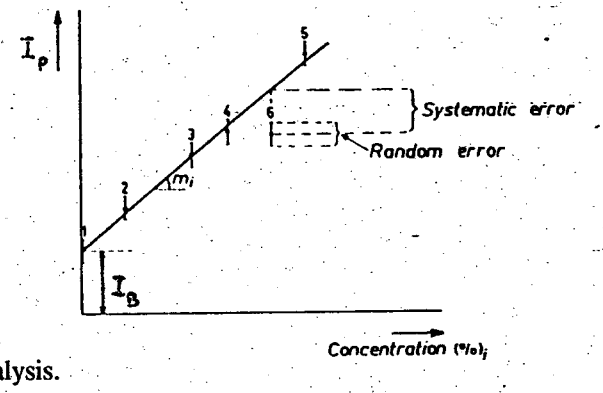

Fig. 18. Random and systematic errors in quantitative analysis.

By a knowledge of the gradient and background intensity I_B the unknown concentration of an element of the sample can be estimated. However, such a linearity applies with the following assumptions.

a) there are no sample effects;

b) absorption is negligible, or the unknown and the matrix have the same absorption for both incident and characteristic X-rays, so that absorption effects do not vary with composition. (Fig.19).

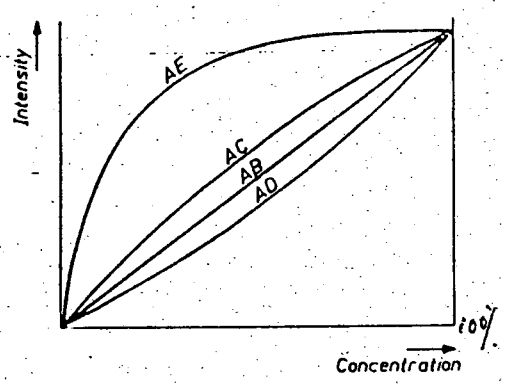

Fig. 19 Effect of absorption on the calibration curve.

Curve	Atomic number of element	Average atomic number of matrix	Example	Range of μ
AB	Medium	Medium	Cu(Kα) in $CuCO_3$ $Ca(OH)_2$	123—133
AC	Heavy	Medium	Pb (Lα) in Sn/Pb	120—138
AD	Light	Medium	Mg (Kα) in Al/5%Cu	735—435
	Medium	Heavy	Sn (Kα) in Sn/Pb	51— 11
AE	Heavy	Light	T.E.L. (PbLα) in gasoline	2—138

c) there is no fluorescent enhancement of one element accompanied by large absorption for another, which would violate condition (b). This happens when two elements near one another in the Periodic Table are contained in the sample.

These three possible causes of non-linearity in the relation between C and I_x are detailed below.

a) Sample effects

i. Lack of homogeneity

ii. Surface irregularity or large particle size. Smearing

iii. Variable density (i.e. compaction). Each of these sample faults leads to variation in the emission of characteristic radiation and errors in the analysis can be up to 100%

iv. Chemical bonding in sample different from that of the standard. This only affects elements from Na to Cl and can lead to a maximum error of 5%.

b) If the linear(/mass) absorption coefficient varies with C, the relationship between C and I_x is no longer linear and either a calibration curve, using a number of samples of known composition, must be constructed or corrections calculated from the elemental composition. Since this is required to be found, the process is an iterative one. Errors from an assumption of linearity can be up to 100%, (in extreme cases).

c) The effect of fluorescent enhancement can be treated in the same way as variable absorption. Uncorrected, it rarely produces errors greater than 10%.

The simple linear relationship usually applies to low concentrations in a light element matrix, e.g. TEL in petrol, or extremely thin samples, such as small volumes of solution evaporated on filter paper, but some alloys, e.g. Fe/Mn, have components with similar absorption coefficients for the characteristic radiation of one or both metals. In general, if the linear absorption coefficient does not vary by more than 5% over the range, and enhancement effects are negligible, a linear relationship will hold within the other errors of the measurement.

Sample effects, in general cannot be corrected for and therefore adequate sample preparation is critically important for accurate quantitative analysis. The other effects can be allowed for mathematically using known absorption coefficients etc. and computer programmes used for the iterative calculations.

We shall now discuss different methods of quantitative analysis.

1. **Linear calibration line method**

As shown in Fig. 19 calibration line is not generally a straight line. However, this is because the concentration range extends broadly from 0 to 100%. If the concentration range is very narrow calibration line can be straight. Therefore if the standard samples are **divided by concentration range**, types of samples, production site or origin, the calibration line will be straight and the analysis will be more precise. Linear calibration curves can be achieved by dilution. In such situations element and matrix range in mass absorption coefficient for the required wavelength does not exceed 5% or so and provided that variation in the concentration of possible enhancing elements is also less than 5%.

2. **Method of reducing matrix effect by dilution**

This is a method of obtaining a linear calibration line after reducing the matrix effect on absorption and fluorescent enhancement by diluting the sample with materials that absorb little X-ray.

For example, when measuring Si Kα in a certain mixtures of SiO_2 and Fe_2O_3, the spread in matrix mass absorption coefficient is 660-1804, a range of 170%. By diluting 9 : 1 with a low absorber, such as lithium carbonate, this range could be reduced to about 16%. The same reduction could, however, also be achieved by a 2 : 1 dilution with a heavy absorber, such as lanthanum oxide.

Since the degree of enhancement is also proportional to the concentration of the enhancing element, it is to be expected that addition of an inert diluent to the matrix would reduce enhancement effects as well.

Dilution methods have been employed with great success over a wide range of applications but probably have been most successful in the analysis of geological samples where elemental concentration ranges can be enormous and where the large number of elements precludes the use of internal standards.

One disadvantage of the dilution method is that complete mixing is absolutely vital. This degree of mixing is best achieved by using the diluent as a solvent for the sample, either as aqueous or acid solutions or by making solid solutions by fusion. In this way it is possible to remove not only the effects of absorption, enhancement and density but also to remove intensity variations attributable to particle size effects. The choice of solvent will of course be determined by the chemical properties of the sample concerned. Although many methods of matrix stabilization by dilution have been successfully employed all suffer from the same fundamental disadvantage - this being that the dilution necessarily reduces the number of analyzed atoms per irradiated volume with a corresponding loss in intensity. This can be particularly troublesome in the analysis of low concentration of light elements where sensitivities may already only be marginally useful.

4. **Standard additive method or Internal Standard (The case of a different element as internal standard)**
Since absorption and enhancement effects are caused by interferences arising from the close proximity of characteristic lines and absorption edges one possible way of overcoming them is to add an internal standard having a wavelength which is affected in a similar manner as the analyzed wavelength. An example might be the determination of iron in Fe_2O_3/Cr_2O_3 mixtures. According to Fig.7 the iron Kα line at 1.937 Å is strongly absorbed by chromium whose absorption edge is at 2.070 Å.

Cobalt has its characteristic Kα line at 1.791 Å and since the absorption of iron and cobalt by chromium is similar. A weighed quantity of, for example, Co_2O_3 could be added to the Fe_2O_3/Cr_2O_3 mixtures as an internal standard.

Since absorption effects for iron and cobalt are similar and as the concentration of cobalt is known.

$$\frac{\text{Count rate due to FeK}\alpha}{\text{Count rate due to CoK}\alpha} = K \frac{\text{Concentration of Fe}}{\text{Concentration of Co}}$$

The calibration factor K could be determined from standard samples of $Fe_2O_3/Cr_2O_3 + Co_2O_3$ and then this factor used in turn to determine iron concentrations in unknown mixtures. It is assumed in this method that particle size and density effects are negligible and particular care must be taken to ensure that the particle size distribution of sample and internal standard are similar. This is why the internal standard method is particularly useful dealing with solutions as they allow a completely homogeneous mixing of sample and standard.

In general the internal standard method is excellent for the determination of single elements in multi-component mixture but is frequently far too tedious for the determination of may elements in the same sample. In as much as the addition of an internal standard entails an extra weighing stage and further mixing, the time involved may be unacceptably long, particularly in case of multiple batch analysis. When dealing with solutions it is sometimes possible to save time by suspending an internal standard block in a sample cup such that it becomes an integral part of the cell. Although this method is somewhat empirical, excellent results have been obtained especially in the analysis of hydrocarbon mixtures for heavy metals.

Using the same element as the internal standard (method of spiking)
When a suitable additive sample cannot be found, it may be possible for the element to be determined as its own internal standard and this can be sometimes more convenient than the use of a different element provided I vs C is linear. Suppose the concentration of unknown be x% and the intensity of the line is I_x. When the element is added by c% let the intensity be I_{x+c} then,

$$(x/100) \div (x+c)/(100+c) = I_x/I_{x+c}$$

If c is small $\frac{x}{x+c} = \frac{Ix}{I_{x+c}}$

From which x can be deduced. This method, which is sometimes known as spiking, is extremely useful for the determination of single elements in very complex matrices since nothing at all need be known about other elements which are present in the sample.In order to obtain reliable results it is necessary that c be of the same order as x otherwise the experimental spread in the measurement of I may influence the slope of the curve, which can lead in turn to erroneous values of x. In order to avoid tedious calculations, the actual weight of added substance should be small compared with the weight of total sample. This is because addition of the amount c to the sample slightly lowers the original value of x. This is one of the reasons why the method of spiking is limited to rather low concentrations, say below 5%. If the correlation between count rate and concentration is not linear, the actual shape of the calibration, line has to be established by repeating the addition, if need be several times. In any event it is best to make a second addition in order to check the linearity of the calibration curve. Again great care must be taken to ensure that the particle size and density of the added element is similar to that of the sample.

Mathematical methods

The incident X-ray is subjected to absorption and the fluorescent X-ray is subjected to both absorption and enhancement. These can be mathematically modelled if the concentration and physical properties of the element and its coexisting elements of the matrix are known. For this purpose it is necessary to have similar surface conditions, density and particle size.

Initially using raw data a calibration curve is established. Since for no absorption and enhancement effects the calibration curve is linear it is possible to get correction coefficients to relate the two curves. These correction coefficients are used with the unknown sample to estimate its true concentration from the raw intensity value. Mere emphasis is now made to use this method in the analysis of multi-element matrices, in preference to more time consuming standard addition and dilution techniques. Mathematical methods will not overcome particle size effects so take care with light elements in powder samples.

Background substraction

Background due to scattered x-rays must be subtracted from a nett peak count for quantitative analysis. Consider X-ray profile of a characteristic line as shown in Fig.20.

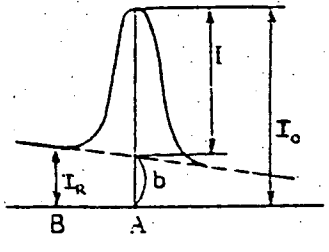

Fig. 20. Compound profile

Assuming that $h = b/I_R$ in the figure at right, the true peak intensity I can be represented by $I = I_0 - h.I_R$

Therefore, is the value of h is evaluated by profiling a standard sample, the actual intensity can be obtained from the above equation by measuring the X-ray intensity of I_R at the point B.

2) Overlap Correction

When two peaks appear closely and partially overlapped, effect of this overlapping is subtracted. Assuming that $k = b/I_R$ in the Fig.21 the true peak intensity I can be expressed by equation;

$$I = I_0 - k.I_R$$

Therefore, when k is evaluated by profiling the standard sample, the true intensity I_R after subtraction of the effect of the element B can be obtained by measuring the intensity I_R of the element B.

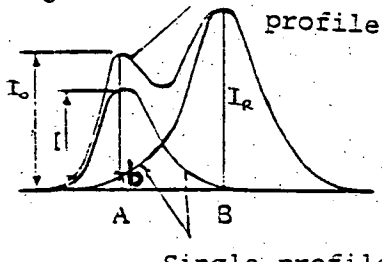

Fig. 21. Single profile

Minimum detection limit (MDL)

The statistical definition of lower limit of detection has been considered by many workers and is normally defined as that concentration which gives a count rate equivalent to background reading plus twice the standard deviation of the background. From this it follows that in the presence of a characteristic radiation this assumption will be incorrect by 5% of cases (95% confidence limit). Where this uncertainty is considered too great a $3\sigma(R_B)$ interval, that is a peak count rate of $R(B) + 3\sigma(R_B)$ is used.

It follows from statistics of count rates $\sigma(R_B) = \sqrt{(B/T_B)}$. Hence $3\sigma(R_B) = 3\sqrt{(B/T_B)}$ cps: which is the nett minimum detectable intensity. Define the slope factor m as the gradient of the I vs C graph. m is cps per sec. Hence minimum detection limit is given by

$$MDL = \frac{3\sqrt{(B/T_B)}}{m} \%$$ This is also approximately equal to

$$MDL = \frac{C_s \, 3\sqrt{(IB)}}{(I_P - I_B)}$$ where I_P is the nett count rate

of the peak and I_B the count rate of the background.

GOOD LUCK AND GOOD ANALYSIS

Rigaku

periodic table of the elements

理学／ポータスペックの分析可能元素は 太ワク の部分です。

1H																	2He
3Li	4Be											5B	6C	7N	8O	9F	10Ne
11Na	12Mg											13Al	14Si	15P	16S	17Cl	18Ar
19K	20Ca	21Sc	22Ti	23V	24Cr	25Mn	26Fe	27Co	28Ni	29Cu	30Zn	31Ga	32Ge	33As	34Se	35Br	36Kr
37Rb	38Sr	39Y	40Zr	41Nb	42Mo	43Tc	44Ru	45Rh	46Pd	47Ag	48Cd	49In	50Sn	51Sb	52Te	53I	54Xe
55Cs	56Ba	57La	72Hf	73Ta	74W	75Re	76Os	77Ir	78Pt	79Au	80Hg	81Tl	82Pb	83Bi	84Po	85At	86Rn
87Fr	88Ra	89Ac															

58Ce	59Pr	60Nd	61Pm	62Sm	63Eu	64Gd	65Tb	66Dy	67Ho	68Er	69Tm	70Yb	71Lu	
90Th	91Pa	92U	93Np	94Pu	95Am	96Cm	97Bk	98Cf	99Es	100Fm	101Md	102No	103Lw	

APPENDIX I

0·10 0·60 1·10

Table of Mass-absorption Coefficients

Z \ λ	0·10	0·15	0·20	0·25	0·30	0·35	0·40	0·45	0·50	0·55	0·60	0·65	0·70	0·75	0·80	0·85	0·90	0·95	1·00	1·05	1·10
1 H	0·28	0·30	0·33	0·34	0·35	0·36	0·36	0·36	0·37	0·37	0·37	0·38	0·38	0·38	0·39	0·39	0·39	0·39	0·39	0·40	0·40
2 He	0·14	0·16	0·17	0·17	0·18	0·18	0·18	0·19	0·19	0·19	0·19	0·20	0·20	0·21	0·22	0·22	0·23	0·24	0·24	0·25	0·26
3 Li	0·12	0·14	0·14	0·15	0·16	0·16	0·17	0·17	0·18	0·19	0·19	0·20	0·22	0·23	0·24	0·27	0·29	0·30	0·32	0·34	0·35
4 Be	0·13	0·14	0·15	0·16	0·17	0·17	0·18	0·19	0·21	0·22	0·24	0·25	0·29	0·32	0·36	0·37	0·42	0·48	0·53	0·59	0·63
5 B	0·13	0·15	0·16	0·17	0·18	0·19	0·21	0·23	0·25	0·28	0·30	0·34	0·40	0·43	0·49	0·57	0·63	0·70	0·78	0·90	0·98
6 C	0·14	0·16	0·17	0·19	0·21	0·22	0·26	0·28	0·34	0·38	0·45	0·53	0·52	0·72	0·81	0·96	1·15	1·30	1·40	1·80	1·80
7 N	0·14	0·16	0·18	0·20	0·23	0·27	0·31	0·37	0·44	0·55	0·63	0·80	0·92	1·05	1·25	1·45	1·70	1·95	2·20	2·50	2·80
8 O	0·14	0·17	0·19	0·22	0·26	0·33	0·38	0·49	0·58	0·72	0·87	1·10	1·30	1·50	1·95	2·40	2·80	3·25	3·75	4·50	5·10
9 F	0·14	0·17	0·19	0·23	0·29	0·38	0·45	0·55	0·72	0·88	1·10	1·30	1·50	1·95	2·40	2·80	3·25	3·75	4·50	5·10	5·80
10 Ne	0·15	0·18	0·22	0·27	0·35	0·43	0·59	0·72	0·98	1·20	1·55	1·90	2·30	2·80	3·45	3·95	4·70	5·50	6·50	7·45	9·65
11 Na	0·15	0·18	0·23	0·29	0·40	0·52	0·71	0·93	1·20	1·45	1·95	2·45	3·00	3·60	4·40	5·25	6·15	7·20	8·35	9·65	11·0
12 Mg	0·15	0·19	0·25	0·35	0·48	0·66	0·91	1·20	1·60	2·05	2·60	3·30	4·10	5·05	6·10	7·30	8·85	10·5	12·5	14·0	16·0
13 Al	0·15	0·20	0·27	0·39	0·56	0·78	1·10	1·45	1·95	2·55	3·25	4·10	5·05	6·10	7·30	8·85	10·5	12·5	14·0	16·0	18·5
14 Si	0·16	0·22	0·31	0·45	0·67	0·96	1·35	1·80	2·40	3·15	4·05	5·20	6·40	7·75	9·20	10·0	11·5	13·5	15·5	17·5	20·5
15 P	0·16	0·23	0·34	0·51	0·77	1·15	1·55	2·20	2·90	3·85	4·85	6·15	7·70	9·35	11·0	13·5	15·5	18·0	21·0	24·0	27·0
16 S	0·17	0·25	0·39	0·61	0·93	1·40	1·95	2·70	3·60	4·65	6·10	7·40	9·10	11·5	14·0	16·0	18·5	22·5	26·5	30·0	35·0
17 Cl	0·17	0·26	0·42	0·68	1·05	1·65	2·25	3·25	4·20	5·50	7·05	8·85	11·0	13·5	16·0	19·0	22·0	26·0	30·5	35·5	40·5
18 Ar	0·17	0·27	0·45	0·73	1·15	1·75	2·50	3·50	4·50	6·10	7·85	9·60	11·5	14·5	18·0	21·5	25·5	29·5	34·0	40·0	46·0
19 K	0·19	0·31	0·54	0·91	1·45	2·20	3·15	4·40	5·95	7·80	10·0	12·5	15·0	18·5	21·0	27·5	32·5	38·5	45·0	52	60
20 Ca	0·20	0·35	0·63	1·05	1·70	2·60	3·80	5·30	7·10	9·30	12·0	15·0	18·5	22·0	27·5	28·0	32·0	39·0	46·0	53	61
21 Sc	0·20	0·37	0·67	1·10	1·80	2·65	3·85	5·40	7·30	9·50	12·5	15·5	19·5	23·5	28·0	32·0	37·0	47·0	54	62	72
22 Ti	0·20	0·39	0·73	1·25	2·05	3·25	4·50	6·40	8·70	11·5	14·5	18·5	22·0	27·0	31·5	40·0	47·0	54	62	72	81
23 V	0·22	0·42	0·80	1·30	2·15	3·30	4·85	6·80	9·10	12·0	15·5	19·0	23·5	28·5	34·5	41·5	48·5	57	65	76	87
24 Cr	0·23	0·47	0·91	1·50	2·65	4·05	6·00	8·75	11·5	15·0	19·0	23·0	29·0	36·0	43·0	52	61	71	83	97	110
25 Mn	0·24	0·50	1·00	1·70	2·70	4·10	6·00	8·40	11·5	15·0	19·0	24·0	29·5	36·5	43·0	54	64	75	86	99	113
26 Fe	0·26	0·56	1·15	2·05	3·35	5·10	7·65	10·5	14·5	19·0	24·0	27·5	33·5	45·5	54	64	75	86	99	110	128
27 Co	0·27	0·59	1·25	2·10	3·50	5·40	7·90	11·0	15·0	20·0	25·5	32·0	40·0	49·0	58	69	82	95	110	122	137
28 Ni	0·30	0·69	1·40	2·60	4·30	6·70	9·70	14·0	18·0	23·5	30·5	37·5	48·0	58	67	76	87	105	122	137	155
29 Cu	0·30	0·72	1·50	2·75	4·55	7·05	10·5	14·5	19·5	24·5	32·0	39·5	44·5	53	65	77	97	112	122	139	158
30 Zn	0·32	0·79	1·65	3·05	5·05	7·75	11·5	16·0	21·5	28·5	36·5	44·5	54·0	65	78	82	100	119	127	143	167
31 Ga	0·35	0·84	1·75	3·30	5·45	8·30	12·0	17·0	22·5	30·5	37·5	47·0	55·0	68	82	100	119	127	143	167	195
32 Ge	0·35	0·89	1·90	3·50	5·85	9·00	13·0	19·0	24·5	31·5	40·5	48·5	60	72	87	107	126	133	152	173	210
33 As	0·39	0·98	2·05	3·85	6·35	9·70	14·0	20·5	26·5	34·5	43·5	55	64	76	91	113	133	141	160	265	30
34 Se	0·39	1·00	2·15	4·05	6·80	10·5	15·0	21·5	28·0	36·5	46·0	56	69	83	97	113	142	151	26	29	33
35 Br	0·42	1·10	2·45	4·50	7·50	11·5	16·5	23·0	31·0	39·5	50	62	76	90	105	127	150	235	27	31	36
36 Kr	0·44	1·20	2·60	4·80	7·95	12·5	17·5	24·5	32·5	42·0	53	65	80	95	109	134	22	26	30	34	39
37 Rb	0·47	1·30	2·80	5·20	8·65	13·5	19·0	26·0	35·0	45·0	57	70	86	101	116	2050	2450	29	33	38	43
38 Sr	0·50	1·40	3·05	5·60	9·35	14·0	20·5	28·5	37·5	48·0	60	75	92	109	19	2250	2650	31	36	41	47
39 Y	0·54	1·55	3·25	6·05	3·95	15·0	22·0	30·0	40·0	50	65	79	99	16	2050	2450	29	34	40	45	51
40 Zr	0·57	1·65	3·50	6·50	10·5	16·0	23·5	33·0	42·5	53	68	84	15	19	2250	27	32	38	43	50	56
41 Nb	0·81	1·75	3·75	6·95	11·5	17·0	25·0	35·5	45·0	57	73	89	16	20	24	2850	34	40	48	54	61
42 Mo	0·65	1·85	4·05	7·45	12·5	18·5	27·0	35·5	48·0	60	75	1450	18	22	26	31	3650	43	51	58	66
43 Tc	0·67	2·00	4·25	8·00	13·0	20·0	28·5	39·0	51	63	105	15	19	2350	28	33	4050	46	56	62	71
44 Ru	0·69	2·00	4·50	8·50	14·0	20·5	29·5	40·0	53	66	13	1650	20	2550	30	36	44	49	59	67	76
45 Rh	0·73	2·15	4·80	9·00	14·5	21·5	31·0	41·5	56	12	15	19	23	28	2350	3950	4650	54	62	72	80
46 Pd	0·80	2·30	5·15	9·45	15·5	23·0	33·0	44·0	57	13	1650	2050	25	31	36	4250	50	58	65	76	87
47 Ag	0·86	2·35	5·50	10·0	16·5	24·5	35·0	47·0	1050	1350	1750	22	27	33	39	46	54	63	73	92	97
48 Cd	0·86	2·45	5·55	11·0	17·5	25·0	35·5	49·0	1100	1450	1850	2350	29	35	4150	49	5750	67	77	38	104
49 In	0·89	2·60	5·80	10·5	18·0	26·0	37·0	300	1200	1550	20	25	3050	3750	4450	4250	61	71	82	94	108
50 Sn	0·97	2·85	6·30	11·5	18·5	27·0	38·5	950	1300	1650	21	2650	3250	40	47	55	65	76	86	101	115
51 Sb	0·99	2·95	6·35	12·0	19·0	28·5	40·0	1000	1350	1750	2250	28	3450	43	50	59	6950	81	93	106	119
52 Te	1·05	3·10	6·75	12·5	20·0	29·0	7·5	1050	1400	18	23	2850	35	44	51	6050	71	83	95	114	127
53 I	1·15	3·35	7·30	13·0	21·0	31·0	8·10	1150	1550	1950	25	31	38	4650	55	6450	76	88	99	120	135
54 Xe	1·15	3·45	7·55	13·5	22	32·5	8·50	12	16	205	26·5	325	405	49	58	69	80	93	112	127	143
55 Cs	1·20	3·55	7·60	14·0	23	6·20	9	12·5	17	22	28	34·5	43	52	61	73	85	99	116	139	156
56 Ba	1·30	3·80	7·75	14·5	23·5	6·50	9·40	13·5	18	23	29·5	37	45	56	65	77	90	106	119	141	158
57 La	1·30	3·80	8·00	14·5	24	6·90	10	14	19	24·5	31	38·5	48	59	69	81	95	111	125	146	166
58 Ce	1·30	3·80	8·20	14·5	24·5	7·40	11	15	20	26	33	41·5	51	61	73	86	100	117	135	155	170
59 Pr	1·35	4·00	8·65	15·5	5·10	7·80	11·5	16	21	27·5	35·5	43·5	54	66	78	91	105	126	143	155	187
60 Nd	1·40	4·15	8·90	15·5	5·40	8·30	12	16·5	22·5	29	36·5	45·5	56	68	81	94	110	130	148	172	195
61 Pm	1·50	4·35	9·25	16	5·60	8·70	12·5	17·5	23·5	30	38·5	47·5	59	71	84	100	115	135	156	179	201
62 Sm	1·55	4·50	9·55	16·5	5·70	8·80	12·5	18	23·5	31	39	48·5	60	73	86	105	120	137	158	181	209
63 Eu	1·65	4·70	9·85	3·70	6·20	9·50	14	19	25·5	33	42	53	65	78	92	110	125	147	169	194	218
64 Gd	1·70	4·85	10	3·90	6·50	9·80	14	20	26	34	43·5	54	66	81	95	115	130	153	176	200	226
65 Tb	1·75	5·10	10·5	4·10	6·70	10	14·5	20·5	27	35·5	45	56	69	84	100	117	135	158	180	233	232
66 Dy	1·85	5·25	11	4·30	7·00	10·5	15·5	22	28	36·5	47	58	71	86	102	122	140	164	187	210	239
67 Ho	1·95	5·45	11	4·40	7·20	11	16	22	29·5	38·5	48·5	61	75	92	107	127	148	173	199	222	251
68 Er	2·00	5·65	11·5	4·50	7·50	11·5	16·5	23	31	40·5	51	63	78	96	113	132	157	180	202	231	261
69 Tm	2·10	5·80	12	4·70	7·80	12	17·5	24·5	32·5	42·5	54	67	83	101	118	141	165	192	211	244	278
70 Yb	2·15	6·10	12	5·00	8·20	12·5	18	25	33·5	43·5	55	59	86	106	123	145	168	197	221	254	288
71 Lu	2·25	6·30	3·00	5·40	8·70	13	19	25·5	35·5	46	59	73	89	109	128	153	178	204	235	269	303
72 Hf	2·30	6·50	3·30	5·70	9·30	13·5	20	27·5	37	47·5	61	76	93	115	135	160	186	219	245	280	
73 Ta	2·35	6·70	3·40	6	9·50	14	20·5	28·5	38	49·5	63	79	97	121	140	166	195	220	250	290	
74 W	2·45	6·90	3·50	6·20	9·90	14·5	21·5	30	40	53	66	83	102	127	148	174	201	230	260		
75 Re	2·55	7·25	3·60	6·30	10	15	21·5	30·5	40·5	53	68	85	104	130	150	177	207	235			
76 Os	2·65	7·45	3·65	6·50	10	15·5	22·5	31·5	42	55	70	87	107	133	155	183	210	245			
77 Ir	2·70	7·65	3·75	6·70	10·5	16	23·5	33	44	57	73	91	113	138	162	192	225				
78 Pt	2·80	7·75	4·25	7·30	11·5	17	24·5	34	47	58	73	92	115	140	165	195	185	148	155	190	90
79 Au	2·90	8·00	4·40	7·45	11·5	17·5	25·5	35	48·5	61	77	96	120	145	170	200	180	156	178	82	92
80 Hg	3·00	2·35	4·65	7·90	12	18	26·5	37	49·5	65	82	103	125	150	185				180	88	93
81 Tl	3·10	2·45	4·80	8·20	12·5	19	27·5	38·5	51	67	85	107	130	155	190				81	92	105
82 Pb	3·15	2·50	4·90	8·25	13	19·5	28	39	53	67	85	108	135	160		125	140	75	85	95	109
83 Bi	3·30	2·55	5·10	8·50	13·5	20·5	30	41·5	56	73	92	117	140	165				79	91	104	115
90 Th	3·25	2·80	5·60	9·40	14·5	22	32	44	59	76	96	76	90	105	75	85	100	116	136	151	168
92 U	3·45	3·25	6·40	11	17·5	27	39·5	55	74	96					80	95	110	127	148	164	180
	0·10	0·15	0·20	0·25	0·30	0·35	0·40	0·45	0·50	0·55	0·60	0·65	0·70	0·75	0·80	0·85	0·90	0·95	1·00	1·05	1·10

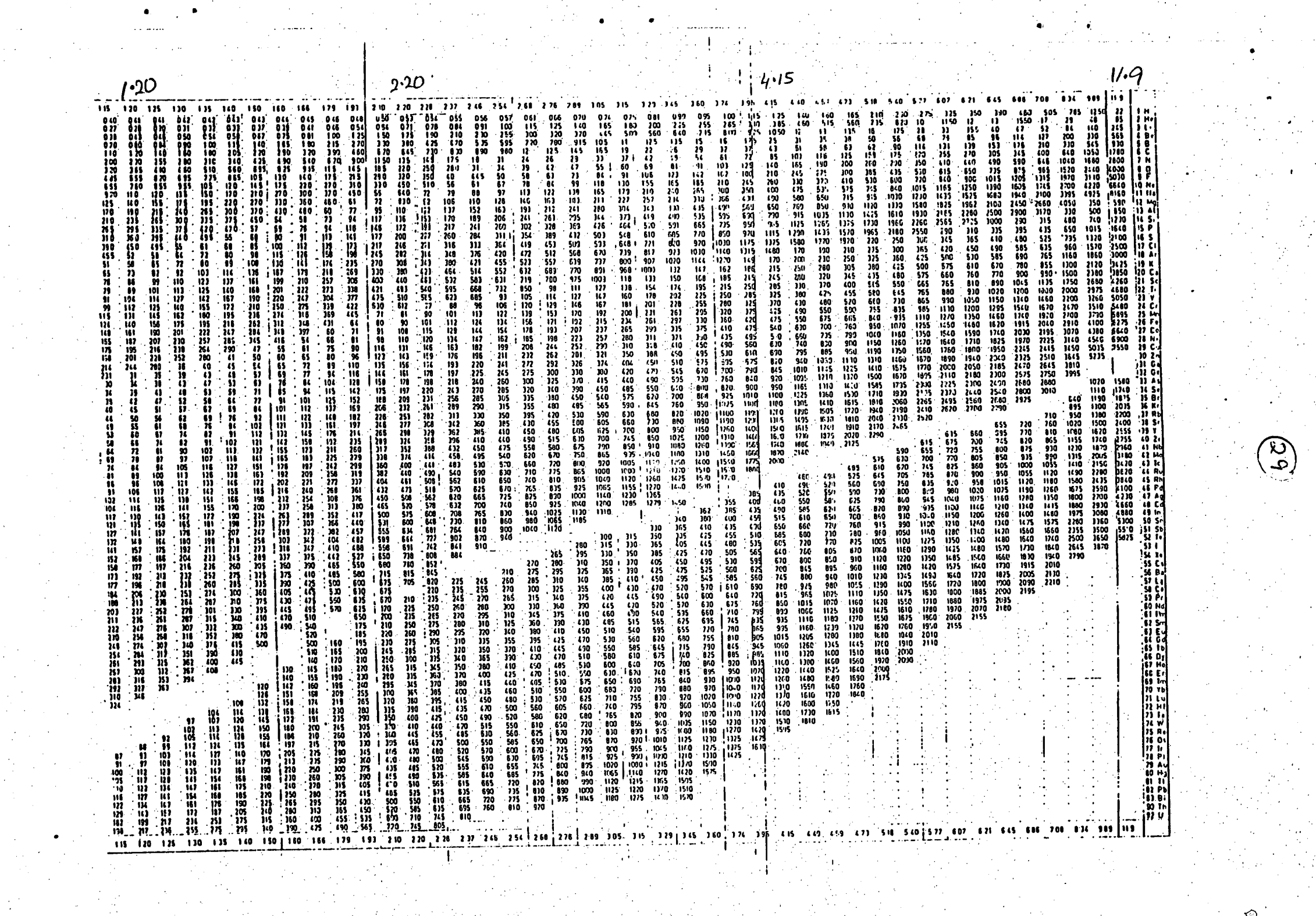
1·20
2·20
4·15
11·9